Pontifícia Universidade Católica
do Rio de Janeiro

Shuai Zhang

Application of graphene oxide and reduced graphene oxide in desalination membranes

Tese de Doutorado

Thesis presented to the Programa de Pós-graduação em Física of PUC-Rio in partial fulfillment of the requirements for the degree of Doutor em Ciências – Física.

Advisor: Prof. Fernando Lázaro Freire Junior

Rio de Janeiro
May 2022

Pontifícia Universidade Católica
do Rio de Janeiro

Shuai Zhang

Application of graphene oxide and reduced graphene oxide in desalination membranes

Tese de Doutorado

Thesis presented to the Programa de Pós-Graduação em Física of PUC-Rio in partial fulfillment of the requirements for the degree of Doutor em Ciências - Física. Approved by the Examination Comittee:

Prof. Fernando Lázaro Freire Junior
Advisor
Departamento de Física – PUC-Rio

Prof. Marcelo Eduardo Huguenin Maia da Costa
Departamento de Física – PUC-Rio

Dr. Suellen Dayenn Tozetti de Barros
Departamento de Física – PUC-Rio

Prof. Yutao Xing
UFF

Prof. Dante Ferreira Franceschini Filho
UFF

Rio de Janeiro, May 6th, 2022

Shuai Zhang

Graduated in physics at Cangzhou Normal University in 2014 and obtained his Mater degree in physics at Hebei Normal University in 2017.

Biliographic data

Zhang, Shuai

Application of graphene oxide and reduced graphene oxide in desalination membranes / Shuai Zhang; advisor: Fernando Lázaro Freire Júnior. - Rio de Janeiro: PUC-Rio, Departamento de Física, 2022.

88 f: il. color. ; 30 cm

1. Tese (doutorado) – Pontifícia Universidade Católica do Rio de Janeiro, Departamento de Física.

Inclui referências bibiográficas.

1. Física – Teses. 2. Osmose reversa. 3. Dessalinização. 4. Membrana. 5. Óxido de grafeno. 6. Óxido de grafeno reduzido. 7. Acetato de celulose. 8. Inversão de fase. I. Freire Júnior, Fernando Lázaro. II. Pontifícia Universidade Católica do Rio de Janeiro. Departamento de Física. III. Título.

CDD: 530

To my mother, for her peace in heaven.

Acknowledgments

This study was financed in part by the Coordenação de Aperfeiçoamento de Pessoal de Nível Superior - Brasil (CAPES) - Finance Code 001. I was also financed by Conselho Nacional de Desenvolvimento Científico e Tecnológico (CNPq) (CNPq – 141179/2019-8).

I would like to thank my Professor Fernando Lázaro a lot. When I feel I was trapped in darkness, his guidance and words always give me strength to go forward.

I also would like to thank Professor Marcelo Maia da Costa. He really helps me a alot in lab and in courses.

Dr. Suellen Tozetti shared massive time with me in lab. We study, research and discuss together. I got countless help from her. I cannot thank her more.

I must thank my friends and colleagues, Dr. Cesar Diaz, Dr. Neileth Stand, Dr. André Barbosa, Dr. Syed Hamza, Pablo Ramón, Dr. Cíntia Aparecida, Dr. Felipe Ptak, Thaís Carvalho, Rodrigo Gomes and Professor Cecilia for their help in my research and daily life.

Thank all the people who shared gorgeous time in PUC-Rio. I would thank Nilton, Sérgio, Carlos Augusto and Édson, they offered a lot supports to me in lab. Thank you PUC-Rio for having me in this excellent university.

Moreover, I would like to thank former director of Confucius Institute of PUC-Rio, Professor Qiao Jianzhen (Ana Qiao) and Professor Yutao Xing from UFF. It's them who introduced this opportunity to me.

Last but not least, I would like to thank my family for their support and love to me. Especially I would like to say "thank you and sorry" to my mother. I didn't take my responsibility for taking care of her. All I could do in the future is never let you down.

Abstract

Zhang, Shuai; Freire Junior, Fernando Lázaro (Advisor). **Application of graphene oxide and reduced graphene oxide in desalination membranes.** Rio de Janeiro, 2022, 88p. Tese de Doutorado – Departamento of Física, Pontifícia Universidade Católica do Rio de Janeiro.

Fresh-water resource scarcity is threatening our society. Urbanization, industrialization, population growth and climate change are making big challenge to human's water resource security. Based on this critical situation, scientists are paying more and more attention to desalination. Traditional desalination methods employ distillation process. These methods play an important role in water supply service in some water-lacked places. However, due to high energy consumption of these methods, the price of produced water is very high. Therefore, developing new desalination technologies with low energy consumption is of high interest and one of them has attracted researchers' attention, which is reverse osmosis (RO).(1) RO utilizes the semi-permeable membrane as a filter, which allows the water or relatively small molecules pass through itself, but prevents the large molecules or ions from penetrate. This technology significantly reduced the energy consumption compared to the distillation methods and quickly takes more than 60% of the total installed desalination capacity.(2) The performance of RO technology strongly depends on the material of membranes plays an important role. In the past decades, polymers, for instance polyamide and cellulose acetate, dominate the semi-permeable membrane RO industry for their good salt rejection efficiency and low cost of energy consumption. However, even with the advantages of polymer membranes, the final cost of produced water is still high. That's why fresh-water resource still remain the concern. Since the first time that graphene was produced from graphite, it caught researcher's attention all over the

world for its ultra-thin 2D structure, excellent conductivity and transparency, etc. Soon after, graphene and its derivatives, such as graphene oxide and reduced graphene oxide, exhibit potential in desalination due to their thin 2D structure and expandability.(3) This work explores the possibility of application of graphene derivatives in a relatively practical desalination process. In the present project, GO (by the Hammer method), RGO (from heating in air atmosphere) and cellulose acetate membranes with GO and RGO were produced. Desalination tests were also performed for samples produced by systematically varying different parameters of GO, RGO and fabrication of cellulose acetate membranes.

Keywords

Reverse osmosis; Desalination; Membrane; Graphene oxide; Reduced graphene oxide; Cellulose acetate; Phase inversion

Resumo

Zhang, Shuai; Freire Junior, Fernando Lázaro (Advisor). **Aplicação de óxido de grafeno e óxido grafeno reduzido em membranas de dessalinização.** Rio de Janeiro, 2022, 88p. Tese de Doutorado – Departamento of Física, Pontifícia Universidade Católica do Rio de Janeiro.

A escassez de recursos de água doce está ameaçando nossa sociedade. A urbanização, a industrialização, o crescimento populacional e as alterações climáticas estão a representar um grande desafio para a segurança dos recursos hídricos humanos. Com base nessa situação crítica, os cientistas estão prestando cada vez mais atenção à dessalinização. Os métodos tradicionais de dessalinização empregam o processo de destilação. Esses métodos desempenham um papel importante no serviço de abastecimento de água em alguns locais carentes de água. No entanto, devido ao alto consumo de energia desses métodos, o preço da água produzida é elevado. Portanto, desenvolver novas tecnologias de dessalinização com baixo consumo de energia é de grande interesse e uma delas tem atraído a atenção dos pesquisadores, que é a osmose reversa (OR). O RO utiliza a membrana semipermeável como filtro, o que permite que a água ou moléculas relativamente pequenas passem por si mesmas, mas impede que as grandes moléculas ou íons penetrem. Esta tecnologia reduziu significativamente o consumo de energia em comparação com os métodos de destilação e rapidamente ocupa mais de 60% da capacidade total de dessalinização instalada. O desempenho da tecnologia RO depende fortemente do material das membranas desempenha um papel importante. Nas últimas décadas, polímeros, por exemplo, poliamida e acetato de celulose, dominaram a indústria de RO de membrana semipermeável por sua boa eficiência de rejeição de sal e baixo custo de consumo de energia. No entanto, mesmo com as vantagens das membranas poliméricas, o custo final da água produzida ainda é alto. É por isso que os recursos de água doce

ainda continuam sendo a preocupação. Desde a primeira vez que o grafeno foi produzido a partir do grafite, chamou a atenção de pesquisadores em todo o mundo por sua estrutura 2D ultrafina, excelente condutividade e transparência etc. Logo depois, o grafeno e seus derivados, como óxido de grafeno e óxido de grafeno reduzido, exibem potencial na dessalinização devido à sua estrutura 2D fina e expansibilidade. Este trabalho explora a possibilidade de aplicação de derivados de grafeno em um processo de dessalinização relativamente prático. No prsente projeto foram produzidos tanto GO (pelo método de Hammer) e RGO (a partir de aquecimento em atmosfera inerte) e de membranas a partir de acetato de celulose com GO e RGO. Ensaios de dessalinação também foram realizados para amostras produzidas variando de modo sistemático diferentes parâmetros de síntese de GO e RGO e de fabricação das membranas de acetato de celulose.

Palavras-chave

Osmose reversa; Dessalinização; Membrana; Óxido de grafeno; Óxido de grafeno reduzido; Acetato de celulose; Inversão de fase

Table of contents

List of figures

List of tables

List of abbreviation

Cellulose acetate (CA)

Dimetilformamida (DMF)

Fourier transform infrared spectroscopy (FTIR)

Forward osmosis (FO)

full width at half maximum (FWMH)

Graphene oxide (GO)

hydrogen peroxide (H_2O_2)

L/m^2*h (LMH)

Multi-effect distillation (MED)

Multi-stage flash (MSF)

nitric acid (HNO_3)

phase inversion (PI)

potassium chlorate ($KClO_3$)

potassium permanganate ($KMnO_4$)

Reduced graphene oxide (RGO)

Reverse osmosis (RO)

sodium nitrate ($NaNO_3$)

sulfuric acid (H_2SO_4)

Thin film composite (TFC)

X-ray photoelectron spectroscopy (XPS)

Where does the right thought come from? Does it fall from the sky? No. Is it inherent in your own mind? No. The right thought can only come from social practice, social production struggle, class struggle and scientific experiment.

Mao Zedong*, Where does the right thought come from?*

1
Development of desalination

In this chapter, current water resource status and desalination's development will be introduced. The materials for desalination membranes, like cellulose acetate and graphene derivatives are introduced too.

1.1
Water resource

Fresh-water resource are becoming more and more critical all over the world. Even though 71% of our planet's surface is covered by ocean, fresh-water only occupies 2.5% of total global water. Moreover, 68.7% of fresh-water is stored in glaciers or ice caps.(4) The shortage of available fresh-water resource turns into a huge problem in modern society.

Urbanization and industrialization are making the situation of drinking water's quality and water supply even worse. According to the research of World Health Organization's research of year 2020, one fourth of the population are facing the problem of lack access to safely drinking water.(5) With urbanization getting faster, particularly more and more people gathering in megacities, water supply and water quality face a big challenge. Furthermore, it's not practical to reduce the pollution significantly in a few years although most people realize the harm of polluted water. Climate change is also considered to increase the risk of drought of water resource on earth surface.

Under this background of global water scarcity, different geometric areas have different difficulties. Most lands of Middle East and North Africa are covered by desert. Approximate 5% of world population lives here. However, it is estimated that 44% of the demand of water supply in these regions' need cannot be met.

Agriculture consumes 84% of available Middle East water resource in Middle EAst. In addition, 98% of agriculture in Middle East relies on regular irrigation. (6) As for Brazil, the situation seems opposite to that of Middle East. Brazil has the largest fresh-water resource, holding 12% of the planet's entire surface sweet water reserves. Amazonia contains most of the country's surface water. However, the population isn't concentrated there but in big cities where people face poor water quality challenge.(7) Besides, some places in Rio Grande do Norte state also face water shortage problem. Both the driest area and the country with the most water resource have their own water resource scarcity problems and the situation is estimated to be worse due to climate change.

Resolving fresh-water shortage problem is a complex and systematic project, which might include improving water utilization efficiency, reducing water resource pollution, building canals, desalination, improving environment and reducing the influence of climate change, etc. This work is intended to improve the desalination process.

1.2
Desalination

Most of the current desalination technologies are divided into two categories: thermal desalination and membrane desalination.

Thermal desalination basically contains two processes, first evaporating salt water and then condensing the steam to gain freshwater. This technology is very classical. In the 4th century BC, Aristotle had already described a thermal desalination technique.(8) However, this technique was premature and only used in some special situations, such as on ships. After industrial revolution, thermal desalination equipment got improved and the very first land-based desalination plants was installed in 1928 in Nederlands Antilles with a production capacity of 60 m^3/day.(9) Subsequently, many desalination plants were built in Middle East. Now the latest thermal desalination plants are based on multi-effect distillation

(MED) or multi-stage flash (MSF) process. This new thermal technology optimizes the energy efficiency significantly comparing to old ones.

On the other hand, RO desalination has a different process. A semipermeable membrane divided two compartments with different concentrated solutions. Water will be driven to pass through the membrane from low concentrate part to the high concentrate part by osmosis pressure, and this process is called osmosis or forward osmosis. In contrast, with a pressure higher than osmosis pressure, applied on the high concentrate part, water from high concentrate part will pass through the semipermeable membrane to low concentrate part. This process is called RO. In 1965, the first RO desalination plant was established. RO desalination plants present immediately a superiority in energy consumption compared to thermal desalination. Until now, with fast development, RO occupied more than 60% of total desalination capacity. Along with years research and development, energy consumption of seawater RO has reduced from 20 kWh/m^3 in 1970s to 2-5 kWh/m^3 today, but still remaining a huge potential to improve energy efficiency.(10)

For reducing energy consumption, some new techniques are proposed in recent years. Forward osmosis (FO) is believed a promising technology to save energy. Unlike RO which needs a high pressure as a driving force, FO utilizes osmosis pressure as the driving force.(11) Because osmosis pressure is caused by pressure difference of two different concentrated liquid, there is need to offer an extra pressure to draw water molecular pass through the membrane. On the other hand, a solution with more concentrated solute than sea water is necessary. In this case, volatile solute, like ammonia and carbonic acid, are very suitable. In FO process, first, dissolve a large amount of volatile solute into the draw solution until that its concentration is more than sea water. Next, put the draw solution and sea water into two chambers which are divided by semi-permeable membrane. Then the water molecular will pass through the membrane by the osmosis pressure from sea water chamber to draw chamber. Finally, heat the draw solution to evaporate the volatile solute and get the final fresh-water product. Even though FO exhibits an excellent benefit in energy consumption, there is still some challenges in choice of draw solution, large-scale use and etc.

This work focuses on RO, which produces fresh water from salty water directly.

1.3
Membrane materials

A good desalination membrane must contain two properties: high water flux and high salt rejection. They are contradictory. Generally, a better water flux means a lower salt rejection, and a better rejection limits water flux. Therefore, finding proper membrane materials for desalination is very important and difficult. Besides, with working time increasing, more and more fouling accumulates on the surface of membrane, which will decrease membrane's water flux and salt rejection. So how such membrane can get recovery via cleaning fouling after a period work becomes important. In industrial use, microorganism always accumulates in membranes' structure.(12) Prevention of the growth of microorganism also should be considered. Now industrial RO membranes are mainly made of cellulose acetate or polyamide.

In the late 1950's, cellulose acetate (CA) was proposed to be used as desalination membrane material by Reid and Breton.(13) The membrane showed a 98% salt rejection. However, its water flux was less than 10 mL m^{-2} h^{-2}, much smaller than practice use.(10) Subsequently, Loeb and Sourirajan made CA membrane possible in practice.(14) From then on, cellulose acetate dominated desalination material for 20 years.

Until the late 1970's, Cadotte and co-workers invented a new polyamide membrane.(15) Their new designed polyamide membranes are prepared by interfacial polymerization. And the polyamide is made into thin film composite (TFC) membranes. TFC membrane consists of three layers: a polyester support layer (120-150 μm thick), a polysulfonic micro-porous interlayer (40 μm thick) and a polyamide ultra-thin barrier layer (0.2 μm thick). This composite structure gives researchers benefits to optimize the functionality of each layer. This new TFC polyamide membrane achieved mort than 99% salt rejection and higher net

pressure driving force which means a larger water flux under the same feed pressure.(16) But it doesn't mean TFC membrane is always with a better flux than cellulose acetate in plant production, the membrane module design also has a significant influence. Herein, this work will ignore industrial design's influence, and focus on properties of membranes.

Now polyamide membranes dominate RO market sales with 91% of total share. (10) Cellulose acetate membranes take the second place, but far behind polyamide. Even though cellulose acetate doesn't have any advantages in salt rejection rate and water flux that are two key factors in desalination, it still has some good properties. Cellulose acetate superior chlorine resistance, which offers prevention of microorganisms' growth by chlorine injection. Cellulose acetate is also an environmentally friendly and relatively cheap material. Besides, cellulose acetate membranes are only made of cellulose acetate which means an easier production process in laboratory.

In industrial use, a small water flux means higher energy consumption. This work will try to explore the possibility to improve the performance of traditional desalination material, like cellulose acetate, and research graphene derivatives' properties in desalination membrane. And for graphene derivatives, cellulose acetate is adopted as base material for forming desalination membrane.

1.4
Graphene and graphene derivatives

In 2004, Andre Geim and Kostya Novoselov extracted one-atom-thick single layer graphene from graphite by mechanical exfoliation (repeated peeling) of small flakes of graphite for the first time.(17) From then on, graphene's unique properties attracted lots of attentions from all over the world. Graphene is a zero-gap semiconductor, because its conduction and valence bands meet at the Dirac points. It even exhibits superconductor property, when bilayer graphene twisted by an angle 1.1° with respect each other.(18) Concerning mechanical properties, graphene is the strongest material ever tested, with an intrinsic tensile strength of 130 GPa (19,000,000 psi) and a Young's modulus (stiffness) close to 1 TPa

(150,000,000 psi).(19) In addition, graphene is impermeable to all gases and liquids.

Graphene's impermeability to water, inspired researchers to drill some pores on its plate to achieve desalination. Through controlling pores' size, only water molecules can pass through the porous graphene. S. Surwade and co-workers bombarded a single layer graphene with oxygen plasma to produce pores.(20) And then they used the porous graphene to filter salt water. Finally, he achieved nearly 100% salt rejection. However, limited by fabrication size of single crystal graphene, the used graphene can only cover 5 μm hole. It is still far away from practice use.

Therefore, graphene's derivative, graphene oxide, was introduced to solve this problem. Graphene oxide (GO) still preserves graphene's honeycomb structure, but is modified by oxidizing groups, such as epoxy, hydroxyl group and carbonxyl group.(21) These groups can crosslink each other, so graphene oxide can be fabricated in a large scale which overcomes graphene's main disadvantage.

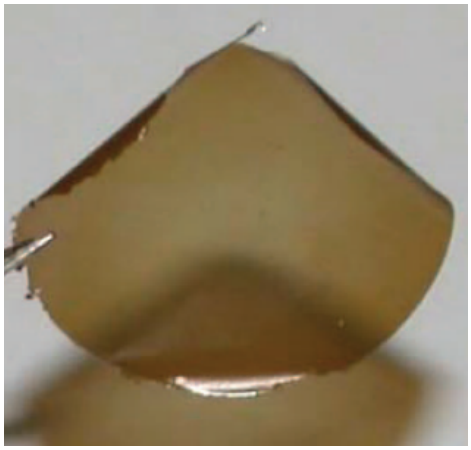

Figure 1: Free-standing graphene oxide layer

GO is fabricated using modified Hummers' method, which generates graphene oxide though a mixture of graphite, sulfuric acid H_2SO_4, sodium nitrate $NaNO_3$, and potassium permanganate $KMnO_4$.(21) Nair and his co-workers have already achieved to synthesize self-supported GO films.(22) They covered a bottle containing water with graphene oxide membrane and measured the evaporate rate.

They found that the evaporate rate of a bottle with graphene oxide membrane is same as the evaporate rate of a bottle without any cover. That means the permeation of water is unimpeded. They speculated that there are two different regions on GO surface, one region is oxidized region with epoxy, hydroxyl or carbonxyl groups; the other is pristine-graphene sheet. Water can pass through the pristine-graphene region quickly, while moves slowly at oxidized region because of hydrogen bonding and a narrow space, just as Figure 2 showed.

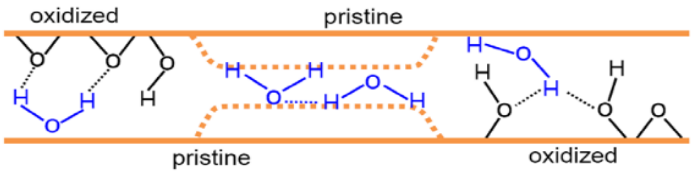

Figure 2: Schematic view for possible permeation through the laminates

Graphene oxide laminates' distance is usually about 0.9 nm. The distance swells to ~13.5 nm in water. But if GO laminates was put at a relative dry condition, distance between laminates would shrink because oxidizing groups would lose water molecular. Once the distance is less than 0.6 nm, it is even difficult for water molecule passing through GO laminates.(23) A possible permeation through the film was given as Figure 3. Jijo Abraham and his co-workers get the similar result through a well-designed experiment. They found they can control GO laminates interlayer spacing through different environmental humidity. Then they glued GO membranes piece by piece and inserted the glued GO bulk into plastic plate to prevent swelling via physical confinement. Finally, they found GO membrane with ~0.64 nm interlayer spacing showed no detectable ion concentration.

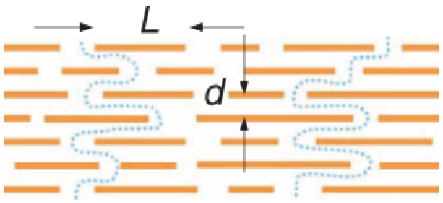

Figure 3: Water molecular through GO laminates

How does ion pass through the membrane? When a salt, such as sodium chloride, dissolves in water, the sodium and chloride ions undergo hydration. Each

individual ion is surrounded by water molecules. The water molecules are polar, with a slight excess of negative charge on oxygen and a slight excess of positive charge on hydrogens. Hydrated ions are larger than it was originally and larger than water molecule, while diameters of common salts are smaller than 0.9 nm, which is GO laminates' distance. So, hydrate ions cannot easily pass through GO laminates.

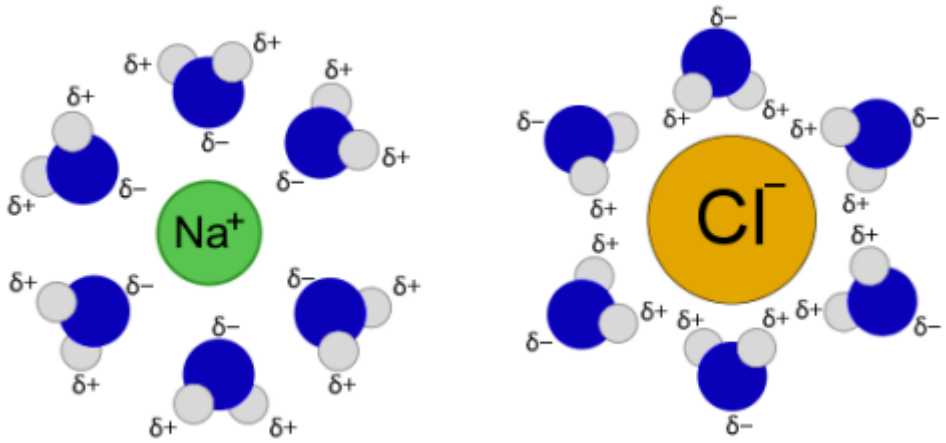

Figure 4: Hydrated sodium ion and hydrated chloride ion

When GO laminates distance is larger than 0.9 nm, hydrated ions will pass the film easily. But if the distance is smaller than 0.9 nm, especially smaller than 0.7 nm, how do ions permeate? Permeating into GO membrane means hydrated ions loose water molecule around it, which may be caused by driving force or membrane inner structure. And then, ions will react with GO. As Figure 5 showed, (24) transition metallic cations interact with the *sp3* C-O matrix via coordination interactions. And alkali or alkaline-earth cations prefer to interact with *sp2* cluster via cation-π interaction. If the distance between GO laminates is reduced, it is more possible that cations interact with GO, in another word, the salt rejection will be enhanced. Once the spacing is reduced to less than 0.7 nm, sodium ion will not pass through GO laminates.(25)

From mechanics of permeation of water and ions through GO laminates, we know that spacing larger than 0.6 nm allows water flux and spacing smaller than 0.7 nm promises ions rejection. So making GO membranes spacing between 0.6 and 0.7 nm is this work's goal.(23) (26) (24) (25) (27)

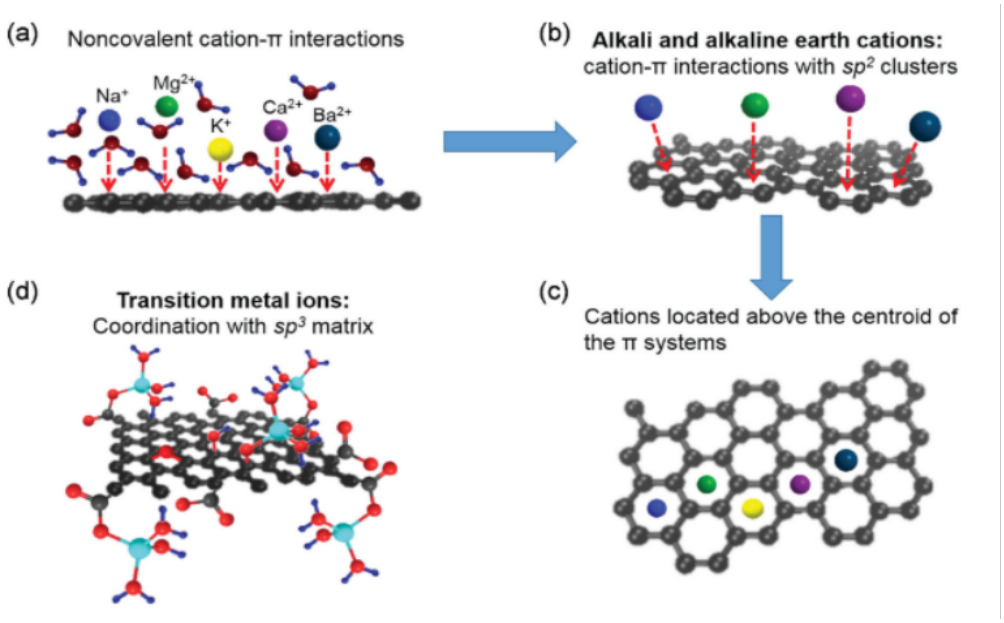

Figure 5: a-c shows alkali and alkaline-earth cations interact with sp2 cluster; d shows transition cations interact with C-O matrix

Therefore, reduced graphene oxide (RGO) seems a natural choice. GO laminates interlayer spacing is too large, because the oxygen groups on GO platelets trap too many water molecules that enlarge GO's inner space. If a part of oxygen groups can be removed from GO laminates, then it might not swell too much. This process is indeed called reduction, so this product material is called reduced graphene oxide. GO can be reduced by thermal reduction, which is used widely for producing RGO. We can control RGO's reduction rate via adjusting temperature and heating time. For producing RGO, 200-300ºC and 1-2 hours are often adopted. RGO laminates interlayer spacing shrinks, because its oxygen groups are removed. Since the oxygen groups on the surface are also removed, as a result, RGO laminates don't link together. Therefore, it's difficult to form membranes with RGO.

In the next chapter, the process of preparing materials and fabrication of different types of membranes will be discussed.

2
Experiment

This chapter introduces the experiment work, which contains preparation of graphene oxide (GO) and reduced graphene oxide (RGO), two kinds of membrane and osmotic system. The two kinds of membrane are vacuum driving memrbane and phase inversion membrane. Both kinds of methods have their own advantages. Vacuum driving membrane benefits from its easy fabrication process and phase inversion membrane is a common method to produce polymer membrane. In the end of this chapter, osmotic system and RO process is introduced.

2.1
Preparation of GO and RGO

2.1.1
Producing method of GO

Despite graphene is a relatively new material, GO's history can be traced back more than 100 years. In 1859, British chemist B. C. Brodie performed a reaction of graphite, potassium chlorate ($KClO_3$) and fuming nitric acid (HNO_3). (28) Brodie determined the resulting material was composed of carbon, hydrogen and oxygen. In 1958, William S. Hummers and Richard E. Offeman created a safer, faster and more efficient method of producing graphene oxide.(29) They abandoned hazardous fuming nitric acid, using concentrated sulfuric acid (H_2SO_4), sodium nitrate ($NaNO_3$) and potassium permanganate ($KMnO_4$) instead.(21) And this method is call Hummers' method. Until now, Hummers' method is still the mainstream technique of producing GO. In this work, Hummers' method is also adopted.

2.1.2
Materials

Materials for preparing GO includes graphite, concentrated sulfuric acid (H_2SO_4), sodium nitrate ($NaNO_3$), potassium permanganate ($KMnO_4$) hydrogen peroxide (H_2O_2) and hydrochloric acid (HCl). Graphite, H_2SO_4, $NaNO_3$ and H_2O_2 were purchased from Sigma-Aldrich. $KMnO_4$ was bought from ISOFAR. The frozen dryer was purchased from LABCONCO, and its model is FreeZone 1.

2.1.3
Process of producing GO

First, 1g graphite and 1.2g $NaNO_3$ was put into a two-necked flask that was then placed on hot plate. Then, stir the mixture of graphite flakes and $NaNO_3$ with stirrer magnet, meanwhile put ice bath (bowl with ice) under the flask. 46 mL H_2SO_4 is then added into the flask in 15 minutes. Next, add 6g $KMnO_4$ into the flask slowly. 5 minutes later, remove the ice bath, and keep stirring for a period of time, which is called “oxidation time”. Oxidation of graphite happens during this time. After oxidation time, 80 mL distilled water was added into the beaker drop by drop. The first 15 mL water should be dropped very slowly to avoid the intense reaction. In this process, the ball capacitor is needed to be inserted into the flask’s neck of gas-released direction. After adding water, the whole solution is moved into a single-neck flask. Then continue dissolving the remaining in the two-necked flask with 50 mL distilled water for three times, and move the remaining solution into the single-neck flask too. After moving the remaining, H_2O_2 was added into the single-neck flask to reduce extra oxidant. Then, leave the system overnight and supernatant appeared. The next day, the supernatant was discarded, and the suspension was divided into six test tubes. 500 mL 4% HCl and were used to wash extra H_2O_2 with centrifuge at 6000 rpm and then distilled water is used to wash the system over and over again until the pH value became 5. In the end, frozen dryer is used to lyophilize the GO suspension. After lyophilization, GO was obtained, and it is dark yellow and in powder form.

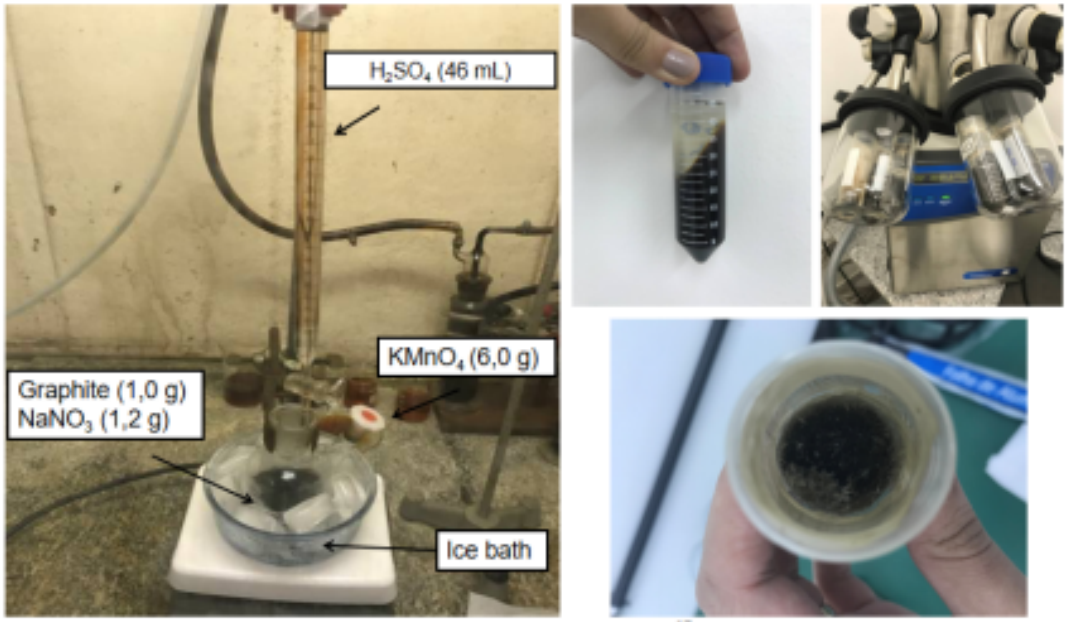

Figure 6: Process of producing GO

2.1.4

Process of producing RGO

GO can be reduced by UV or sunshine treatment, reducing agent and thermal reduction that is used in this work.

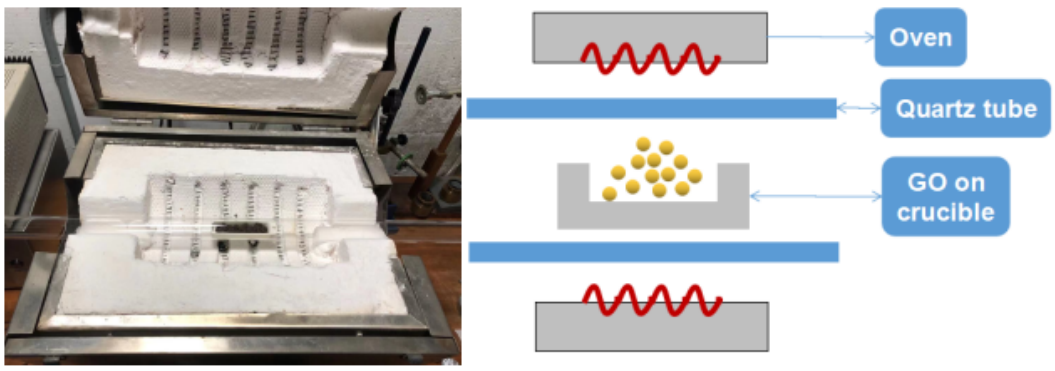

Figura 7: RGO in oven and produce scheme

The only material for producing RGO is GO. And the only equipment needed here is electric oven. The process of producing RGO is putting graphene oxide powder into electric oven under 200ºC for a period of time which is called reduction time and is used to obtain different RGO with different degree of reduction. The obtained RGO is black, and in powder form.

2.2
Vacuum driving membrane

GO can dissolve into water because of massive oxygen groups attached on GO's plates. So it is possible to make a membrane via filtering GO suspension with a filter paper under vacuum driving. The filter used in this work is purchased from TJ-Jinteng. The material of the filter is nylon 6 and the pore size is 0.22μm.

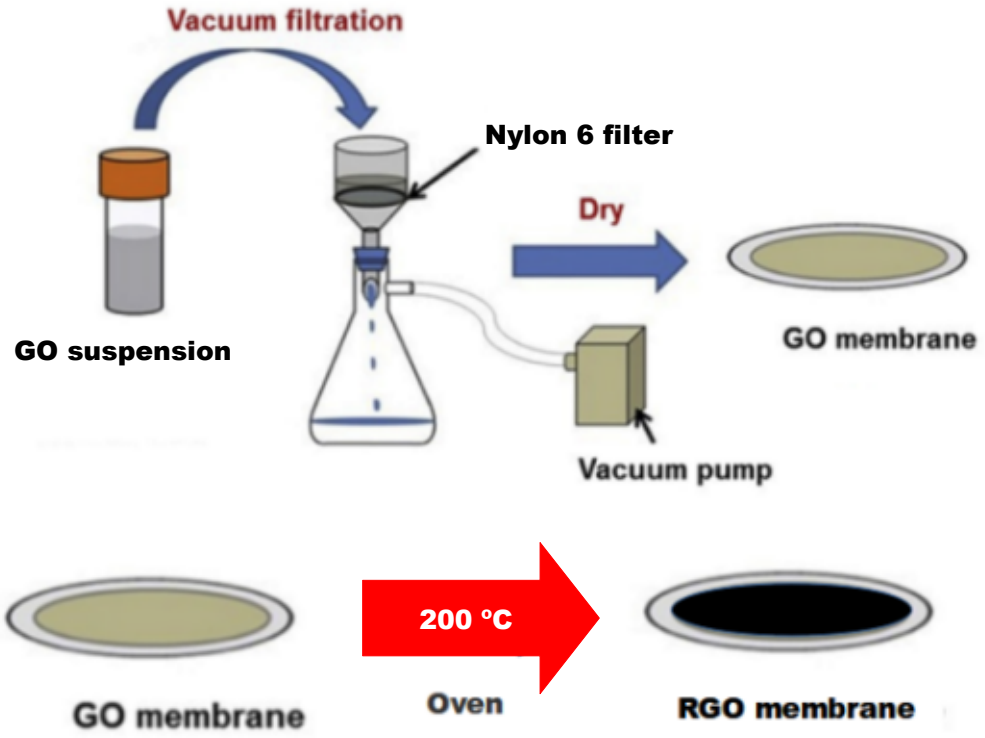

Figure 8: RGO Preparation scheme

GO vacuum driving membrane is composed of two layers: the upper layer is GO layer; the lower layer is the filter paper. Because of the good solubility of GO, GO layer on filter is very easy to be peeled by water flow during testing process. Therefore, medical tape (sticky medical bandage) is here used to cover the GO layer to protect the GO layer from peeled away. The medical tape is purchased from 3M Nexcare and its material is viscose rayon non-woven with hypoallergenic acrylic adhesive. The pore size in this tape is unknown, but the tape can let water to pass through it easily without any salt rejection. So the final vacuum driving membrane consists of three layers: the upper layer is madical tape layer; the middle layer is GO layer; the lower layer is filter paper.

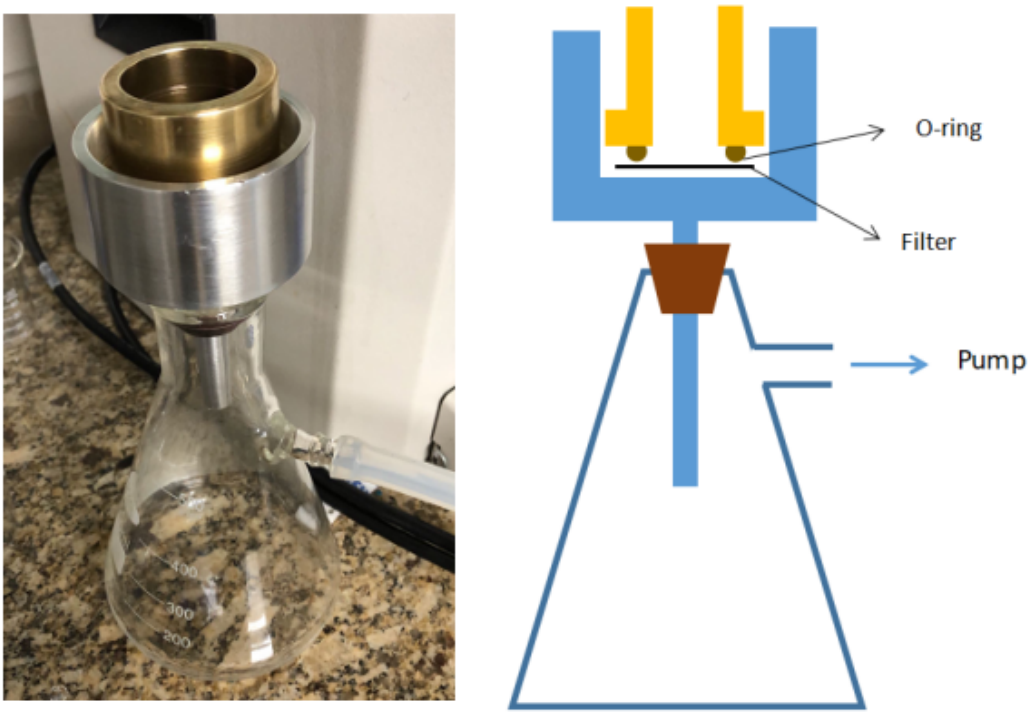

Figura 9: Scheme of producing GO vacuum driving membrane

As for RGO, it doesn't dissolve into water. We can't make the RGO vacuum driving membrane like GO. Filtering RGO suspension cannot form a RGO layer, instead we will see RGO powder loosely stacked on the filter above funnel's pore. RGO membrane is made through reducing GO vacuum driving membrane at 200ºC in electric oven. GO vacuum driving membrane without medical tape is put into electric oven to reduce the GO on the filter. The reduction condition is the same as the RGO powder. After reduction, RGO vacuum driving membrane is obtained.

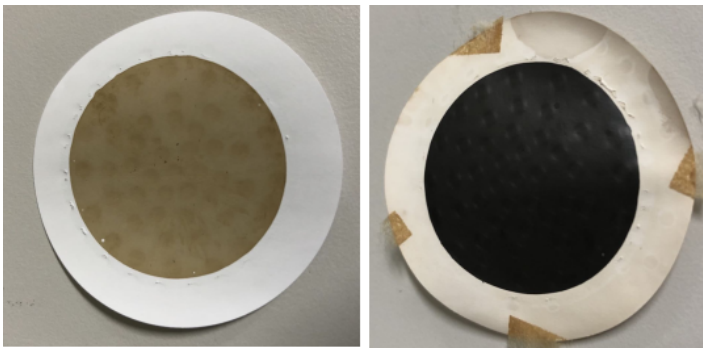

Figure 10: GO and RGO vacuum driving membrane

2.3
Phase inversion membrane

2.3.1
Phase inversion

Phase inversion is a common method to prepare polymeric membranes. Phase inversion describes a phenomenon in which dissolved polymer in solution become precipitating and forming membrane when polymer's solubility decreases. It may occur in different situations, for instance: immersing polymer solution into anti-solvent; reducing the temperature of solution; evaporating the solvent in air or at high temperature; exposing the polymer solution to a vapor anti-solvent and other situations that could reduce the polymer's solubility.

In this work, immersing polymer solution into anti-solvent is adopted for its easier variable controlling and potential for large scale production.

2.3.2
Cellulose acetate membrane

Herein, cellulose acetate is used as the polymer forming final membrane, acetone and Dimetilformamida (DMF) are used as polymer's solution and distilled water is used as anti-solvent.

First, cellulose acetate dissolves into mixture of acetone and DMF. Then, the mixed system is stirred with magnetic stir bar overnight. Next, stop the stirring,

and let the mixed homogeneous solution stand for 1 hour to debubble. After above steps, the solution is ready to use.

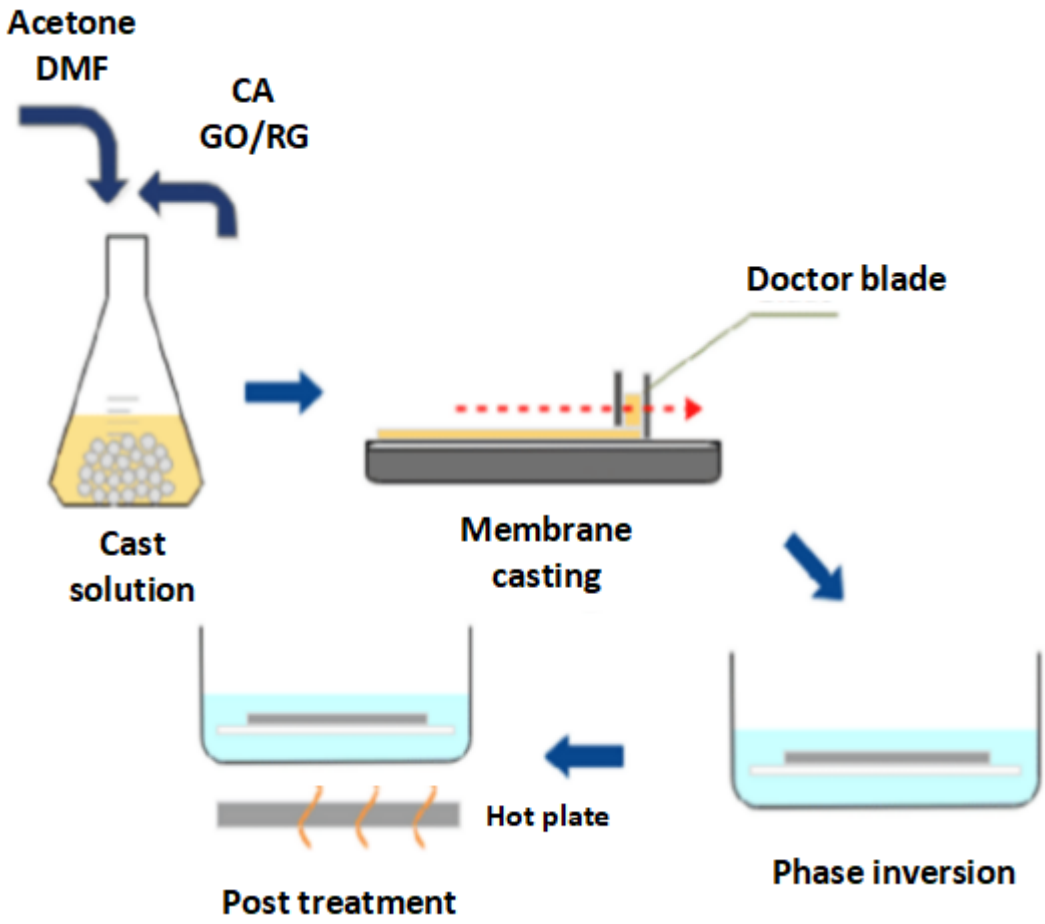

Figure 11: Phase inverse membrane casting process

Next steps are setting casting system. Doctor blade, which has a flat edge and is a component of printer, is used here to cast the solution on a flat glass plate. The doctor blade is connected with two height adjusters which consists of a screw and a spring with a scale division 20 μm. Height of doctor balde can be controlled by adjusting the two screws. To ensure that the doctor blade and glass plate are operated on flat, they are put on a bigger flat thick glass base.

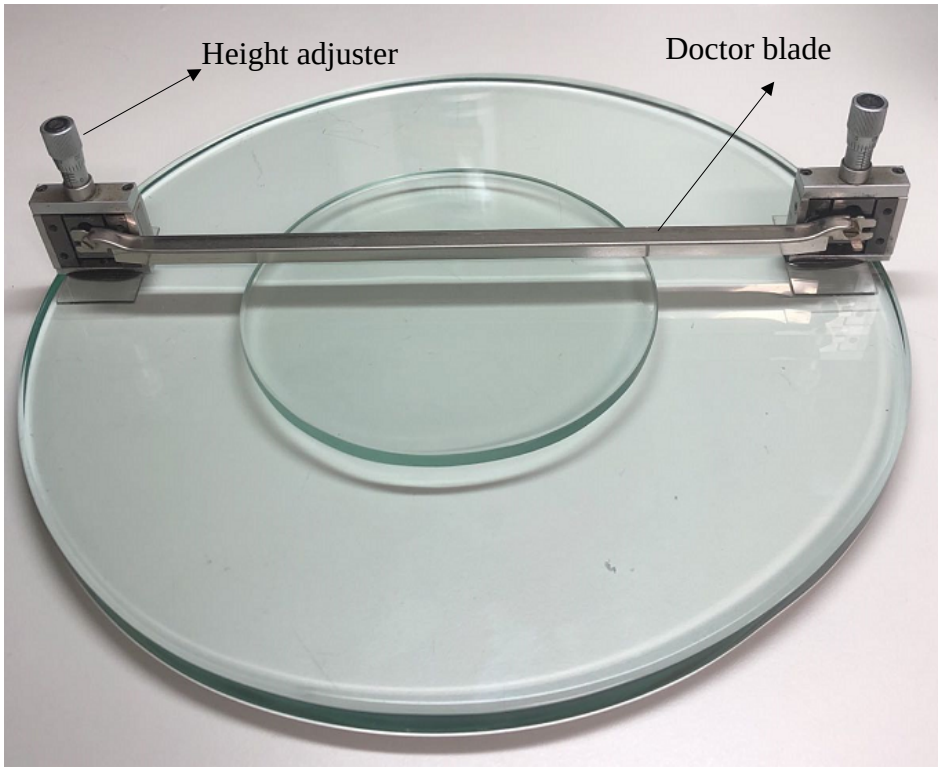

Figure 12: Membrane casting system

Next step is calibrating the height adjusters. When the doctor blade is slightly touching the glass plate, the calibration is ready, and the height is set as 0. Then increase the height to a determined value that is also the membrane's initial thickness.

Pour the cellulose acetate solution onto the glass plate, and cast the solution with doctor blade. Then, expose the casting solution in air for a period of time, which is evaporation time and is discussed in chapter 4.2.4. During this period of time, volatile solvent, here it's acetone, will evaporate. So the upper layer solution has more concentrated solute, in contrast, the inferior layer solution has dilute solute.

Now prepare a big vessel with ice water. Put the glass plate with casting solution into ice water. The solvent (acetone and DMF) will exchange with non-solvent (water) in the solution structure. In this process, porous structure will form. After the solvent dissolve into water, the solution gets solidified. The upper layer, which used to have more concentrated solute, forms a dense layer that is usually called skin layer. The inferior layer, which used to have dilute solute, forms a sub-layer with macrovoids (tear-like or finger-like structure). The faster the process is, the more macrovoids sub-layer has. Skin layer offers a higher rejection and worse

flux. In contrast, the sub-layer with macrovoids offers a better flux and worse rejection.

Figure 13: From left to right: two pure CA membrane, GO-CA membrane and RGO-CA membrane

The final step is post treatment that is hot water bath treatment. High temperature makes membrane shrink, and pore size in the membrane shrinks too. This step influences membranes' performance significantly, particularly the salt rejection. The operation is moving the membrane from ice water into hot water bath.

Therefore, in fabrication process, we can use either evaporation time, hot bath temperature and hot bath time to adjust the membranes' performance.

2.3.3
CA-GO or CA-RGO membranes

For CA-GO or CA-RGO membranes, the process of producing is similar to that of cellulose acetate membrane. The only difference is that in first step, GO or RGO should be dissolved into solvent. And then exfoliate the GO or RGO with ultrasonic cleaner for hours until obvious stack of GO or RGO disapears. It generally takes about 3 hours to exfoliate GO and about 6 hours to exfoliate RGO. After that, put the cellulose acetate into the solution. Subsequent steps are same as cellulose acetate membranes.

2.4
Osmotic system

For osmotic systems in laboratory, there are two types of systems we can choose. One is called head-end osmotic system; the other one is cross-flow osmotic system.

Head-end osmotic system is made of a pressure provider and a membrane cell. The pressure provider can be a water pump or a high pressure cylinder and supplies pressure on the membrane cell which contains solution in itself. Pressure pushes the solution to pass through the membrane that is put on the end of the cell. The penetrating liquid through the membrane is final product liquid. The head-end osmotic system is relatively easier to build up. However, salt accumulates heavily on the surface of membrane and forms fouling during the osmosis process. Especially for long time running, the accumulated salt is an obvious negative impact to permeate flux.

Cross-flow osmotic system has a different mechanism. The key component of cross-flow system is a set of circulation loop tubes that connect pump, water tank and membrane cell. Pump draws water from water tank and offers power to water to flow along tubes back to water tank. Membrane cell is attached on the loop tubes. The direction of water flow in tube is tangential to the membrane's surface, rather than perpendicular to the surface in head-end osmotic system. In the circulation process, a small part of water will pass through the membrane under the driving pressure. Because of water's circulation and parallel position of water flow and the membrane's surface, fouling is going to accumulate much slower in cross-flow system than in head-end system.

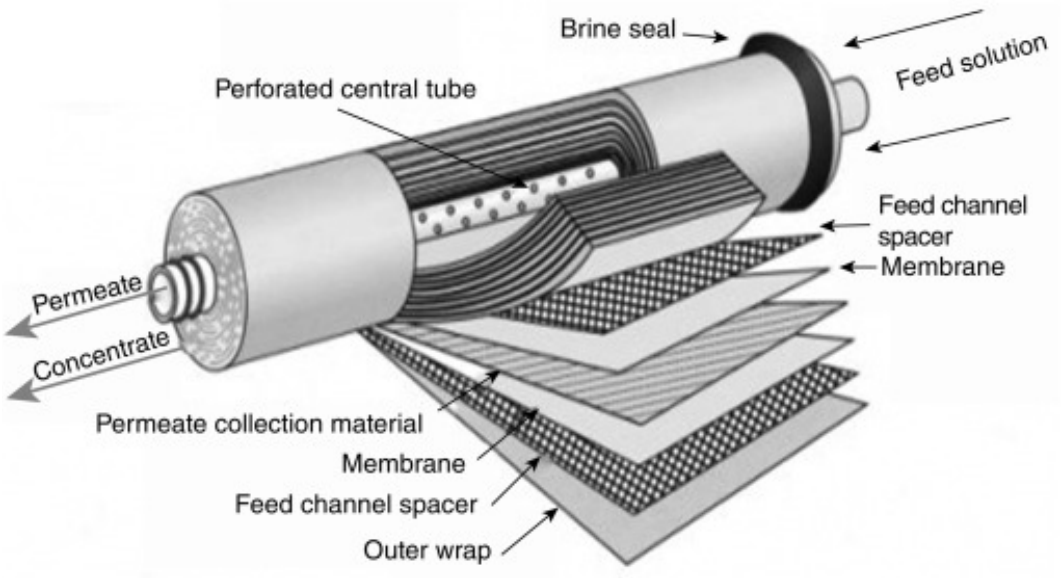

Figura 14: Commercial RO membrane cylinder

Current RO desalination plates also adopt head-end osmotic system. The membrane cell used is RO membrane cylinder that contains a large scale of RO membrane rolled over and sealed in it. This design increases membranes' area and permeate efficiency and decreases fouling on membranes' surface due to head-end osmosis mechanism.

Figure 15: Cross-flow membrane cell. Water goes into the membrane cell from the blue point and goes back to tank through the red point. The filtered water goes out the system from green point.

Therefore, in this work, head-end osmotic system is utilized to test membranes' performance. Besides, it is not necessary to fabricate a membrane cylinder at laboratory scale. A normal small flat membrane is enough for testing.

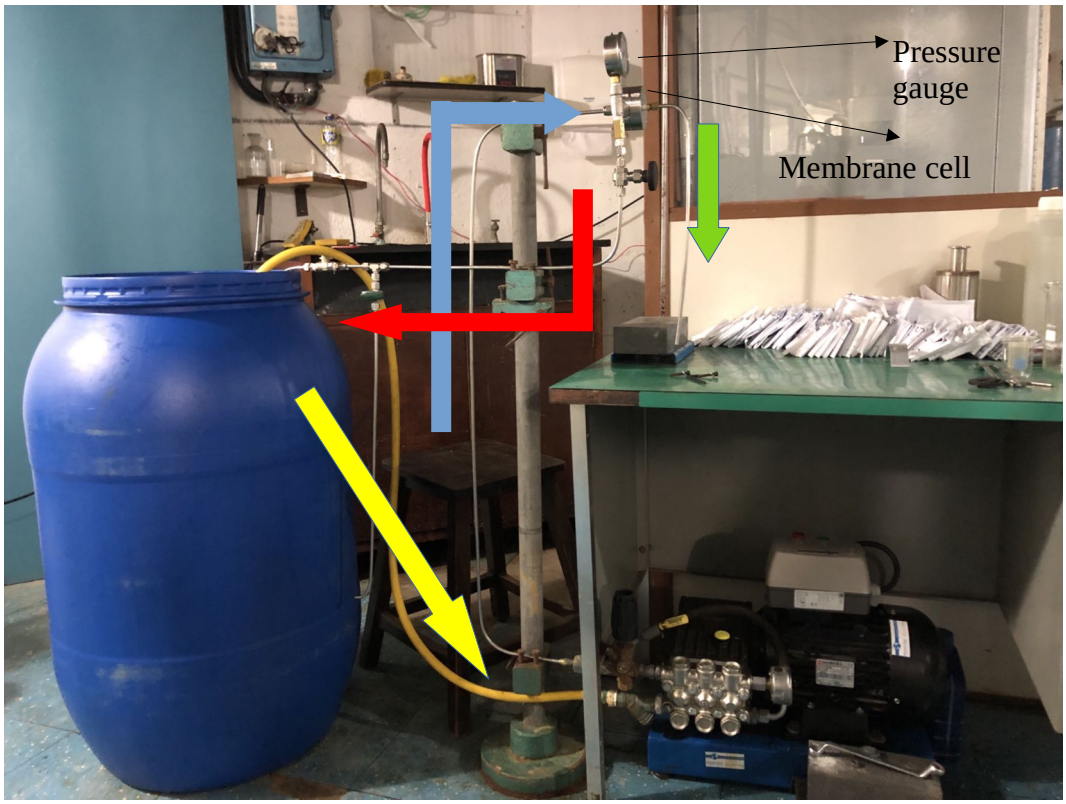

Figure 16: Cross-flow osmotic system. Water is drawn by pump along the yellow tube (yellow arrow), and go up into the membrane cell (blue arrow). Some water goes through membrane (green arrow) and majority water goes back into the water tank (red arrow).

The cross-flow osmotic system used in this work is shown in figure 16. The blue big barrel is the water tank whose maximum capacity is 100 L. Because the water pump generates too much heat during its operating, the water temperature will get very high which is a damage to the water pump. In experiments, 20 L water at room temperature can be heated up to around 50-55ºC in 1-hour running. Larger amount of water can extend the operation time significantly. In membranes' tests, 60 L water is adopted. The running time is from half hour to five hours, depending on the permeate flux. Besides, the feed solution in the tank is NaCl solution with a 3000 ppm concentration. The water pump is on the ground, shown in the figure 16. It was purchased from MundoAzul (Model: W916 montada). Its maximum working pressure is 160 Bar. In membranes' tests, 10 bar is used as the driving power. The membrane cell is attached on the circulation tube above the desk. It

has one entrance and two outlets: one leads back to water tank, the other lead filtered water out the circulation loop.

In osmotic process, water is drawn by the pump from the water tank to flow through the entrance of the membrane cell. And then, in the membrane cell, water flows tangentially along the membrane and goes back to the water tank. At the same time, a small part of water penetrates the membrane and arrives in the beaker on the desk. And this small part of water is the filtered water. There is a tap between the membrane cell and water tank. It can help to adjust the pressure through controlling the water flux in the loop (The pressure adjusting handle on the water pump is the main means.). If the tap is closed totally, the cross-flow osmotic system will turn into a dead-end osmotic system. Of course, the overheating and fouling problem will be more significant.

Flux was calculated with equation:

$$J_v = \frac{V}{A \times t}$$

Here, V is volume permeate through the membranes; A is membranes' effective area; t is work time. The unit is L/m^2*h. This unit is often written in short as LMH.

Salt rejection was calculated with equation:

$$R(\%) = \left(1 - \frac{C_p}{C_f}\right) \times 100\%$$

Here, C_p is salt concentration of permeate and C_f is salt concentration of feed solution.

In experiments, NaCl solution is used as feed solution, and its concentration is set as 4000 ppm. The pump's working pressure is 10 bar. Salt concentration was measured by conductivity meter. The conductivity meter is calibrated with 1000 ppm NaCl solution. The sensor of conductivity meter should contact with target solution well during measurement.

3
Characterization of GO and RGO

This chapter introduces the characterization of GO and RGO. Fourier transform infrared spectroscopy (FTIR), Raman spectroscopy and X-ray photoelectron spectroscopy (XPS) are used to investigate GO and RGO. FTIR reveals bonds' changes with along with oxidation and reduction, especially expoxy bond's increasing of in oxidation and decreasing in reduction. Raman reveals graphene's plate structure's dignity through comparing the ratio of D-band to G-band and the full width at half maximum (FWMH) after oxidation and reduction. XPS reveals the change of contents of carbon and oxygen and the change of C-O bond and C=O bond, which recalls the analysis of FTIR.

3.1
FTIR spectra of GO and RGO

FTIR utilizes the interactions of infrared radiation with molecules, functionalities and chemical bonds. These interactions absorb certain frequencies that are characteristic of their chemical structure. The vibrational or rotational energy of chemical bonds, molecules or atoms matches the infrared radiation, especially the mid-IR range 400-4000 cm^{-1}.(30) Through recording its absorption of infrared radiation, sample's functional groups(31)(32)(33) or adsorbates(34) information can be estimated. FTIR only takes a short time and small amount of sample to get a spectrum. FTIR techniques are used to characterize oxygen functionalities, which are important for analysis of GO and RGO.

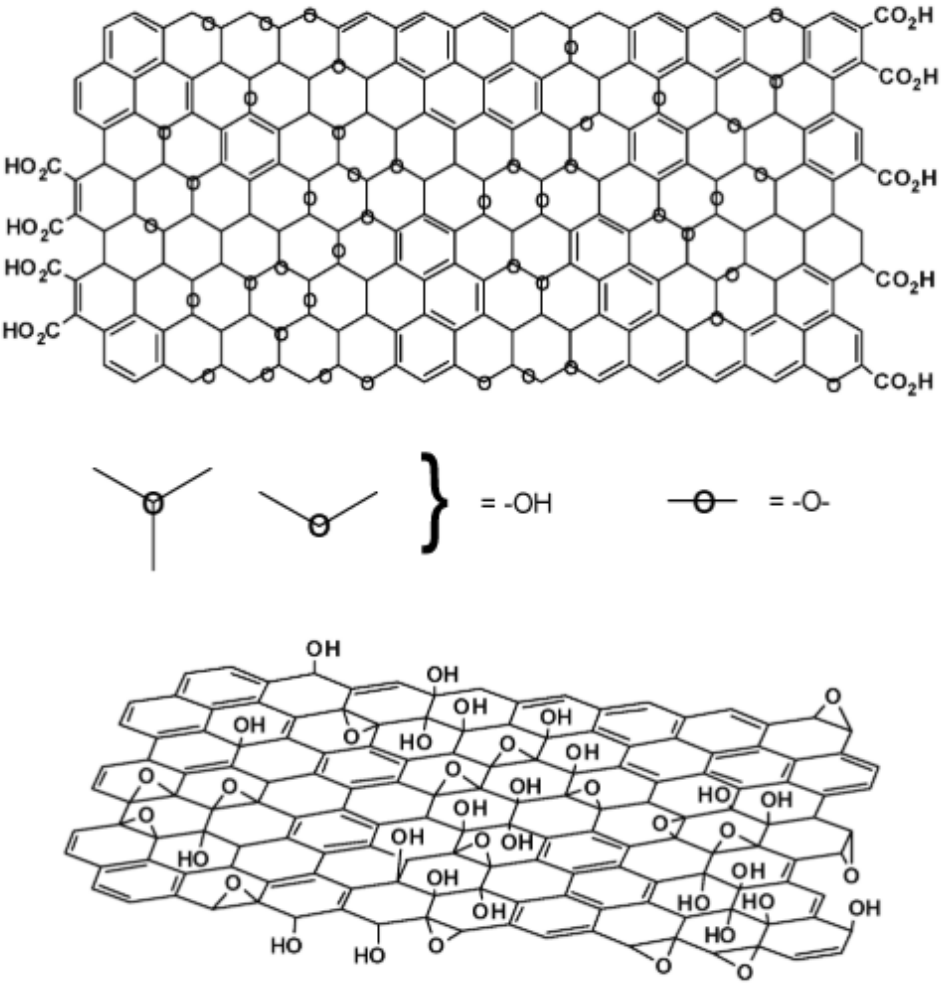

Figure 17: Graphene oxide's structure of the Lerf-Klinowski model , oxygen functionalities attached on graphene's plate

Graphene oxide can be simply understood as some functional groups attached on graphene's plate.(35)(36) These groups include carboxyl, epoxy, hydroxyl, carbonyl and etc. They are indicated by the characteristic bands of FTIR spectrum. Hydroxyl bands are at 1070 cm^{-1} and 3050-3800 cm^{-1}; Epoxy (C-O-C) band is located on 1230-1320 cm^{-1}, and epoxy or peroxide's (C-O-C) band appears at 957 cm^{-1}; the O-H deformation is at 1404 cm^{-1}; Sp^2-hybrided C=C bond is at 1500-1600 cm^{-1}; Ketonic species (C=O) are at 1600-1850 cm^{-1}, especially carboxyl (-COOH) is at 1650-1750 cm^{-1}.(37)(38)(39) Functionalities of GO with their own position in FTIR spectra are listed on table 1. The FTIR spectrometer used here is "Fourier transform infrared spectroscopy, model ALPHA, Bruker".

Table 1: Characteristic vibration modes and their energies

Wavenumber (cm^{-1})	Function group
3050-3800	-OH
1600-1850	C=O
1650-1750	-COOH
1500-1600	C=C
1404	O-H
1230-1320	C-O-C
1070	-OH
957	C-O-C

3.1.1

FTIR of 5 different GO samples

GO0.5h, GO1h, GO2h, GO5h and GO1D, corresponding to GO with different oxidation time. Their codenames and corresponding times are listed on table:

Table 2: List of five GO samples with different oxidation time for FTIR characterization

Codename	Oxidation time
GO0.5h	0.5 hours
GO1h	1 hour
GO2h	2 hours
GO5h	5 hours
GO1D	1 day

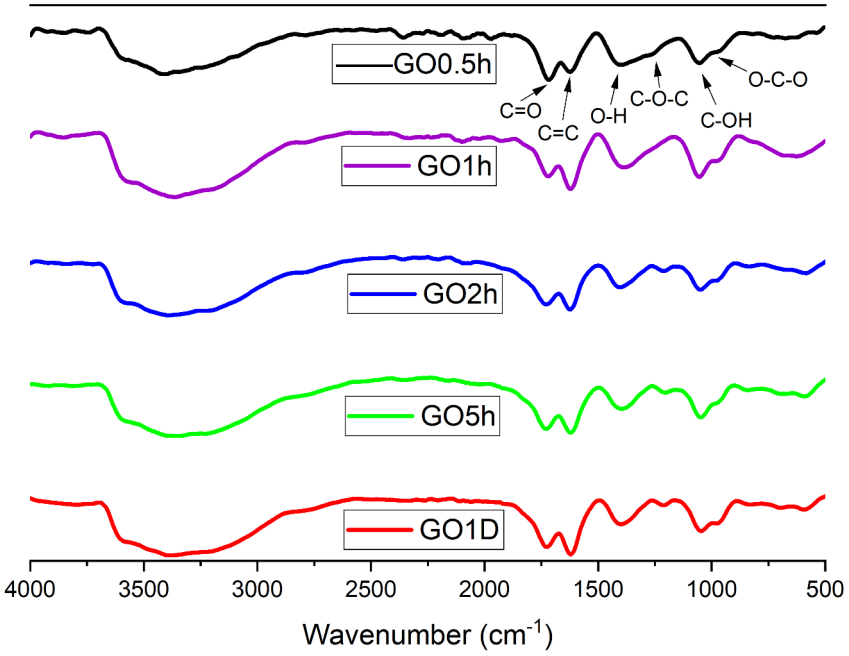

Figure 18: FTIR spectra of GO0.5h, GO1h, GO2h, GO5h and GO1D

From these 5 graphene oxide samples' FTIR spectra, we can see that carboxyl, hydroxyl, epoxy groups exist in GO samples with different oxidation time. Epoxy band (1230-1320 cm^{-1}) become sharper along with oxidation time's increasing. Even epoxy's another possible band 957 cm^{-1} becomes very clear on GO1D, in contrast, the presence of the band at 957 cm^{-1} is not obvious for GO0.5h. And hydroxyl's band 1404 cm^{-1} of GO0.5h is smaller than the other GO samples with longer oxidation time. It seems that more oxygen groups were attached on the four GO samples than on sample GO0.5h. The change of other functional groups seems very tiny.

3.1.2

FTIR of GO2h sample and RGO samples reduced from GO2h

For exploring the reduction's influence, GO2h and RGO samples reduced from GO2h are characterized by FTIR. The RGO samples are reducd at 200ºC for

different reduction time. Samples Codenames and responding reduction time of tested samples in this section are listed in table:

Table 3: List of GO2h and RGO samples reduced from GO2h with different reduction time for FTIR characterization

Codename	Reduction temperature	Reduction time
GO2h	200ºC	0
RGO 200C 1h of GO2h	200ºC	1 hour
RGO 200C 2h of GO2h	200ºC	2 hours

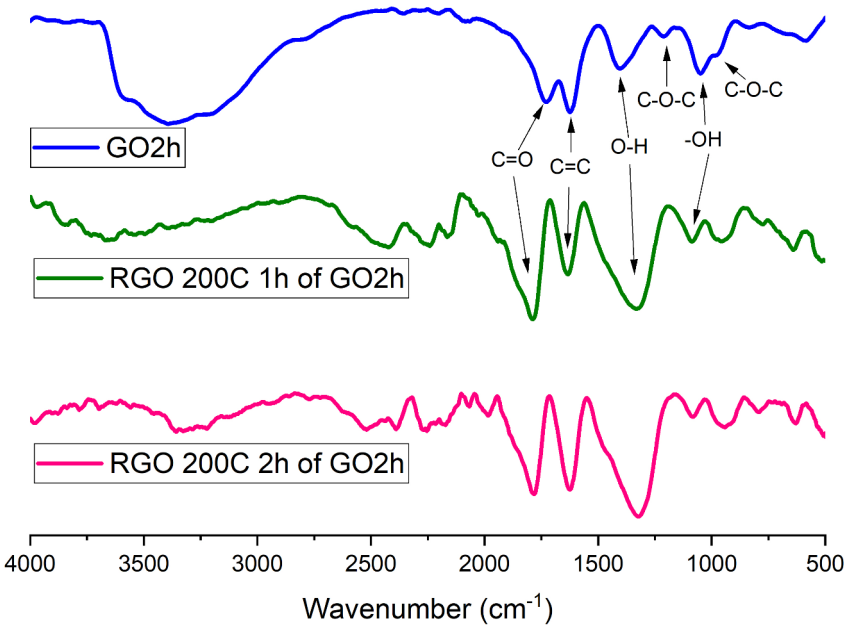

Figure 19: FTIR spectra of GO2h, RGO 200C 1h of GO2h and RGO200C 2h of GO2h

Figure 19 shows the FTIR spectra of GO2h, "RGO 200C 1h of GO2h" and "RGO200C 2h of GO2h". From the spectra, we can find that epoxy group (1230-1320 cm^{-1}) disappeared in two RGO spectra after reduction and C=C, C=O and O-H bands become more clear. At 300-3500 cm^{-1}, the huge -OH band is much flatter than GO2h. One other band worthy to be mentioned is the C=C band in RGO 200C 2h of GO2h. Because this band is more obvious than 1hour RGO.

3.1.3

FTIR of GO1D sample and RGO samples reduced from GO1D

In last section, GO1D and RGO samples reduced from GO1D are characterized by FTIR and compared. These RGO samples are reduced at 200ºC. There codenames and responding reduction time is listed in table

Table 4: List of GO1D and RGO samples reduced from GO1D with different reduction time for FTIR characterization

Codename	Reduction temperature	Reduction time
GO1D	200ºC	0
RGO 200C 1h de GO1D	200ºC	1 hour
RGO 200C 2h de GO1D	200ºC	2 hours
RGO 200C 3h de GO1D	200ºC	3 hours

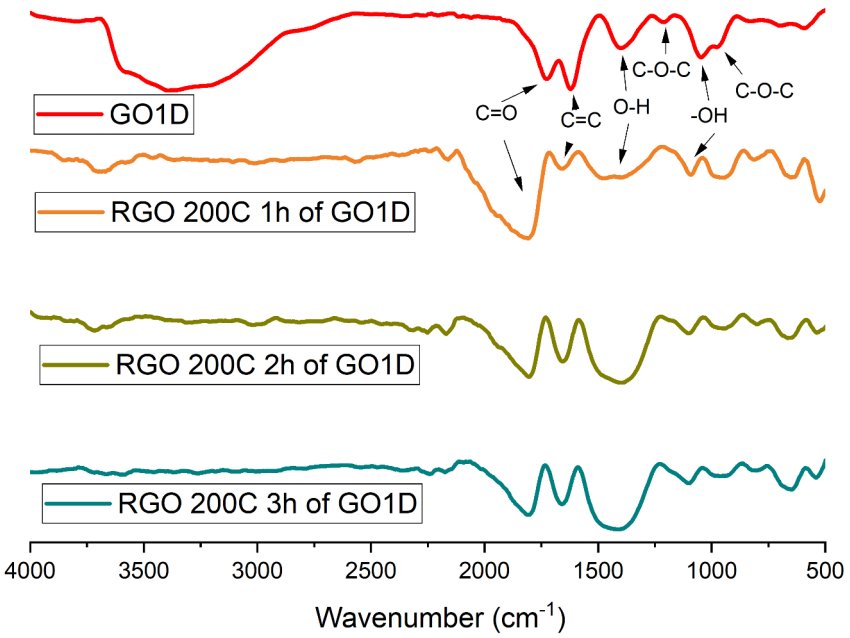

Figure 20: FTIR spectra of GO1D, RGO 200C 1h of GO1D, RGO 200C 2h of GO1D and RGO 200C 3h of GO1D

Similar to GO2h and its RGO samples, RGO samples, obtained from reduction from GO1D, lose their C-O-C band. C=O and C=C bands become bigger and

wider. Among these three RGO, “RGO 200C 1h of GO1D” reserves more similarities with GO1D than the other two. Its O-H band is not as tall as the others’ and its C=C band is less obvious.

At 3500 cm^{-1}, “RGO 200C 1h of GO1D” and “RGO 200C 2h of GO1D” still reserve a small band. However, the band of RGO 3h of GO1D is almost flat in 3500 cm^{-1}. It means that RGO samples lose more water attracted in graphite laminates with increasing reduction time.

Comparing “RGO 200C 1h of GO1D” and “RGO 200C 1h of GO2h”, it is clear that “RGO 200C 1h of GO2h” reserves less features than its counterpart. The reason might be that GO1D carries more oxygen groups than GO2h, therefore, after the same period of reduction time, the RGO of GO1D reserves more GO’s feature.

3.2
Raman spectra of GO and RGO

Raman spectroscopy measures vibration, rotation and other low-frequency modes. It is also commonly used in analyzing chemical structures of carbon materials.(40)(41)(42)(43)(44)(45)

Raman and FTIR spectroscopy are similar. Raman can offer us the chemical information through scattering of light. Raman spectroscopy depends on a change in polarizability of a molecule, whereas IR spectroscopy depends on a change in the dipole moment. Therefore, they can provide complementary structural information. Especially, for carbon materials, carbon skeleton has a high Raman activity while functional groups have high infrared activity.(46)

In Raman spectrum of carbon materials, G-band (graphite band) represents an ideal graphite lattice vibration mode with E_{2g} symmetry, and this band is located at about 1580 cm^{-1}. Materials with oriented graphite structure are often shown a relatively high intensity G-band. After oxidizing graphite, the G-band is broadened. That indicates that the graphene lattice is destroyed.(30)(47) D-band is another important band for carbon materials, and it appears at about 1350 cm^{-1}, corresponding to a graphite lattice vibration mode with A_{1g} symmetry. D-band is a

defect-induced Raman feature and cannot be seen for a highly crystalline graphite. (48) The ratio of I_D/I_G is normally used to describe the degree of disorder for graphitic materials. The model of Raman spectrometer is NTEGRA Spectra, NT-MDT. The used laser's wavelength is 473 nm. CCD temperature is -50ºC and measurement time for each sample is 60 seconds.

3.2.1

Raman spectra of 4 different GO samples

In this section, graphite and four GO samples, GO2h, GO3h, GO5h and GO1D, are characterized by Raman spectroscopy. Their codenames and corresponding oxidation time are listed in table 5:

Table 5: List of graphite and four GO samples with different oxidation time for Raman characterization

Codename	Oxidation time
Graphite	0
GO2h	2 hours
GO3h	3 hours
GO5h	5 hours
GO1D	1 day

Comparing the Raman spectra of all kinds of GO and graphite, we can find that after oxidation, the G-band in spectra of GO get broadened, while the D-band get taller and broadened too. Then according to the ratio of D-band to G-band, we can find that the ratio increases along with increasing of oxidation time. That means the GO gets more disordered along with increasing oxidation time.

Table 6: Information of Raman spectra of graphite, GO2h, GO3h, GO5h and GO1D. Peak center, FWHM and ratio I_D/I_G are shown in the table.

Codename		Graphite	GO2h	GO3h	GO5h	GO1D
D	center	1365.0	1363.6	1358.8	1361.6	1359.5
	FWHM	108.6	185.9	177.8	172.3	190.4

G	center	1582.7	1582.6	1580.7	1579.3	1580.7
	FWHM	28.4	92.0	80.6	80.6	82.2
I_D/I_G		0.64	1.53	1.99	1.94	2.05

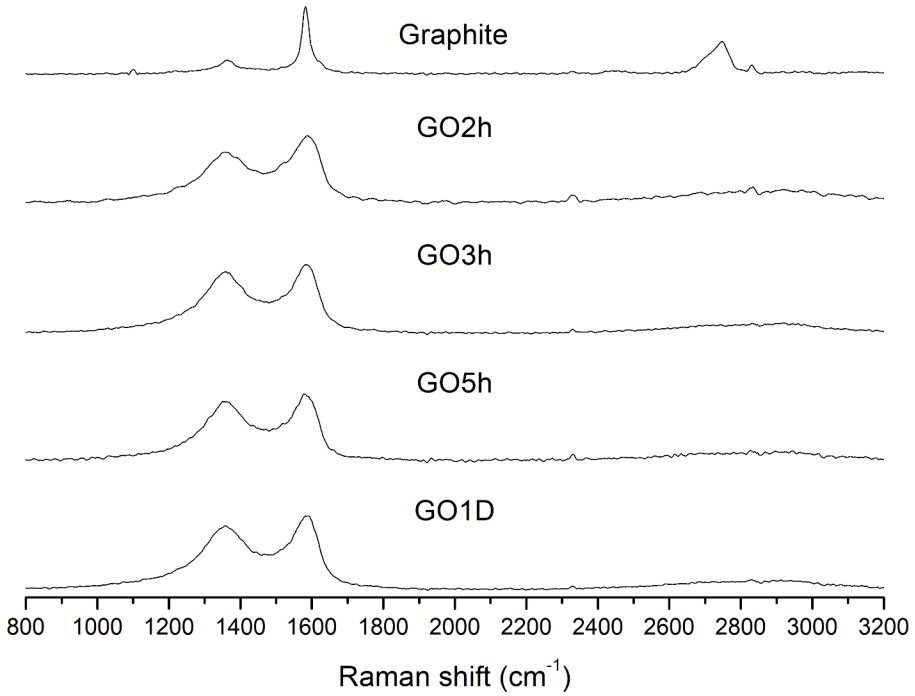

Figure 21: Raman spectra of graphite, GO2h, GO3h, GO5h and GO1D

3.2.2

Raman spectra of GO2h sample and RGO samples reduced from GO2h

In this section, GO2h and two RGO samples reduced from GO2h are characterized with Raman spectroscopy. The RGO samples are reduced at 200ºC for different reduction time. Their codenames and corresponding reduction time are listed in table 7:

Table 7: List of GO2h and RGO samples reduced from GO2h with different reduction time for Raman characterization

Codename	Reduction temperature	Reduction time
GO2h	200ºC	0
RGO 200C 1h of GO2h	200ºC	1 hour
RGO 200C 2h of GO2h	200ºC	2 hours

Table 8: Information of Raman spectra of GO2h, RGO 200C 1h of GO2h and RGO 200C 2h of GO2h. Peak center, FWHM and ratio I_D/I_G are shown in the table.

Codename		GO2h	RGO 200c 1h of GO2h	RGO 200c 2h of GO2h
D	center	1363.6	1363.9	1363.2
	FWHM	185.9	193.4	175.2
G	center	1582.6	1584.5	1585.2
	FWHM	92.0	84.9	85.8
I_D/I_G		1.53	1.95	1.75

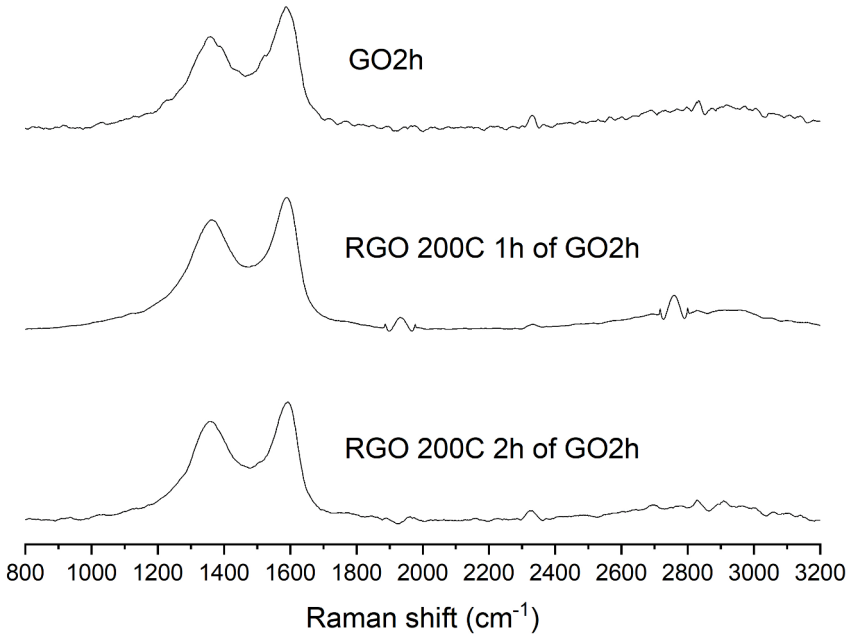

Figure 22: Raman spectra of GO2h, RGO 200C 1h of GO2h and RGO 200C 2h of GO2h

According to the ratio I_D/I_G from table 8, it increases along with increasing reduction time. That may mean graphene's structure is damaged during the reduction procedure. However, I_D/I_G of "RGO 200C 2h of GO2h" are smaller than "RGO 200C 1h of GO2h", indicating that may mean GO's plate structure recovers a little to graphene structure after functional groups were removed from GO's

plate. A more important indication on this direction is the reduction of the FWHM of the G-band.

3.2.3

Raman spectra of GO1D sample and 5 RGO samples reduced from GO2h

In this section, GO1D sample and five RGO samples reduced from GO1D are characterized with Raman spectroscopy. The RGO samples are reduced at 200ºC from GO1D for different time. Their codenames and corresponding reduction time are listed in table 9:

Table 9: List of GO1D and RGO samples reduced from GO1D with different reduction time for Raman characterization

Codename	Reduction temperature	Reduction time
GO1D	200ºC	0
RGO 200C 0.5h of GO1D	200ºC	0.5 hours
RGO 200C 1h of GO1D	200ºC	1 hour
RGO 200C 2h of GO1D	200ºC	2 hours
RGO 200C 3h of GO1D	200ºC	3 hours
RGO 200C 5h of GO1D	200ºC	5 hours

Table 10: Information of Raman spectra of GO1D, RGO 200C 0.5h of GO1D, RGO 200C 1h of GO1D, RGO 200C 2h of GO1D, RGO 200C 3h of GO1D and RGO 200C 5h of GO1D. Peak center, FWHM and ratio I_D/I_G are shown in the table.

Codename		GO1D	RGO 200c 0,5h of GO1D	RGO 200c 1h of GO1D	RGO 200c 2h of GO1D	RGO 200c 3h of GO1D	RGO 200c 5h of GO1D
D	center	1359.5	1358.6	1355.3	1358.1	1357.3	1357.0
	FWHM	190.4	168.0	173.8	167.6	167.2	174.3
G	center	1580.7	1581.2	1578.4	1582.5	1580.3	1580.4
	FWHM	82.20	78.6	80.1	77.1	79.4	78.5

I_D/I_G	2.05	1.97	1.95	1.98	1.93	2.03

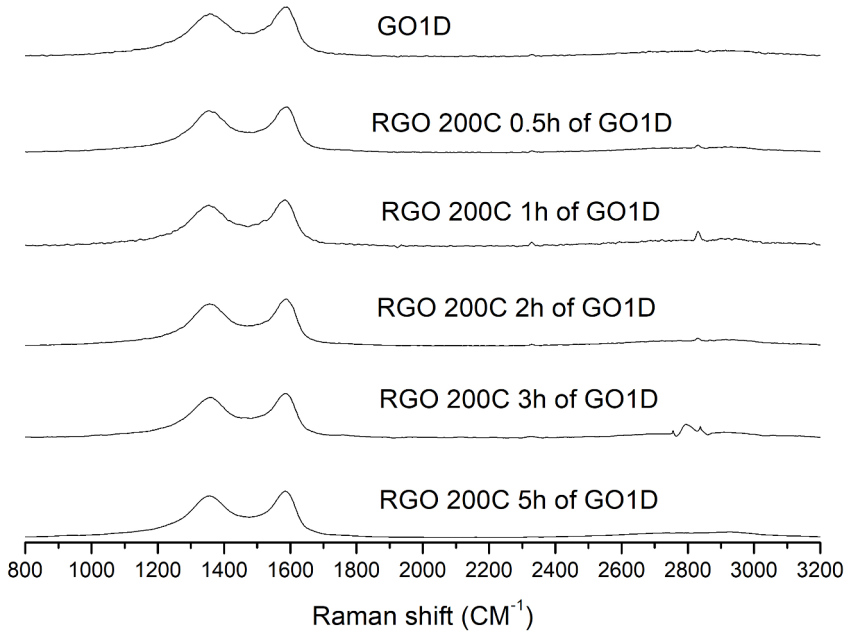

Figure 23: Raman spectra of GO1D, RGO 200C 0.5h of GO2h, RGO 200C 1h of GO2h, RGO 200C 2h of GO2h, RGO 200C 3h of GO2h and RGO 200C 5h of GO2h

From the spectra and analysis table, we can find that the ratio I_D/I_G almost doesn't change after reduction. That may mean the GO1D's graphene plate is heavily damaged. Even though the functional groups are reduced, the degree of disorder doesn't change.

3.3
X-ray photoelectron spectroscopy

XPS, X-ray photoelectron spectroscopy, can provide materials' information about its element content and its valence state. Through irradiating a sample with X-ray and measuring the number and kinetic energy of the escaping electrons from the surface of the material, XPS spectra is obtained. XPS can reflect the content and the chemical state of the surface elements.(49)(50)(51) Because the depth X-ray can penetrate is very limited, XPS is a surface sensitive analysis method. Generally, XPS can get materials' information from 0-10 nm depth.

For GO and RGO, they are carbon materials with functional groups attached. Therefore, carbon and oxygen are the main elements to detect. C*1s* XPS peak (binding energy) of spectra of carbon materials is from 280 to 300 eV. More specifically, C-C (including C=C) is at 284.6 eV; C-O signal is at 286.7 eV and C=O signal is at 288.9 eV.(52) As for O*1s* XPS peak, it isn't as clear as the C*1s* is. C=O is located at 530.7-532.2 eV and C-O is at 533.0-534.6 eV.(53)

From XPS spectrum, information of elements' atomic percentages and each element ambient (chemical bonds) can be gotten from data analysis. In the following content of this chapter, GO and RGO samples' XPS spectra are analyzed. And spectrum for each sample includes survey, C*1s* and O*1s*. Electron spectra are measured by a hemispheric analyzer, VG Thermo Alpha 110. The x-ray source is from magnesium (Kα=1253.6 eV). The data is analyzed by software CasaXPS with background type Shirley and line shape Gaussian-Lorentzian GL(40) for deconvolution.

3.3.1
XPS spectra of 4 different GO samples

In this section, GO1h, GO2h, GO3h and GO5h are characterized by XPS. GO samples characterized here are listed at table 11:

Table 11: List of 4 GO samples with different oxidation time for XPS characterization

Codename	Oxidation time
GO1h	1 hour
GO2h	2 hours
GO3h	3 hours
GO5h	5 hours

According these GOs' XPS survey results, we can find that the content of carbon and oxygen in these GO samples almost doesn't change. Carbon corresponds about 66 at.% while oxygen content is about 33 at.%. Similar results were also obtained from the C*1s* and O*1s* spectra. For all the GO spectra in C*1s* and O*1s* regions, both bonds' positions and contents don't change with increasing oxidation time. In C*1s* spectrum, C-O bond has a sharper peak than the other two peaks, which corresponds to about 50% of the total C present at the sample, while C-C corresponds to about 40% and C=O to about 10%.

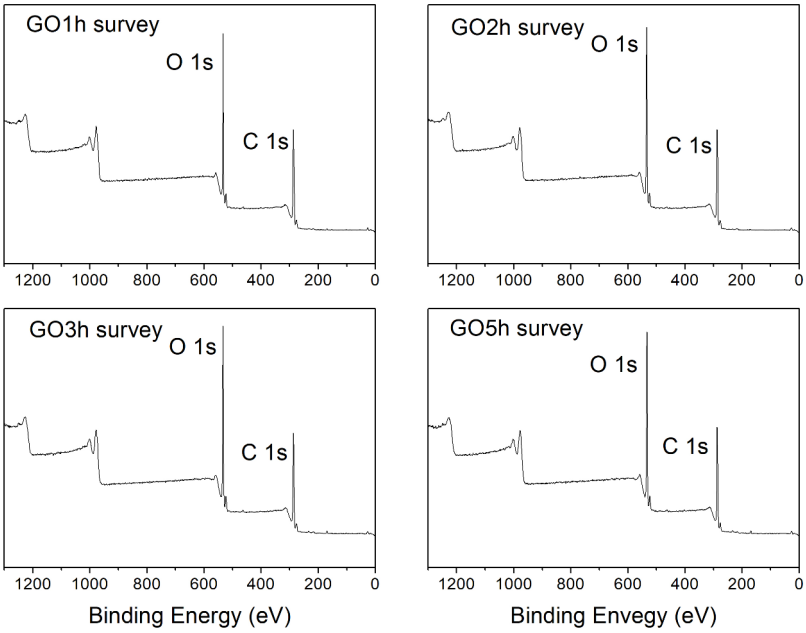

Figure 24: XPS survey spectra of GO1h, GO2h, GO3h and GO5h

Table 12: Information of contents of C1s and O1s from XPS survey spectra GO1h, GO2h, GO3h and GO5h

Codename	C*1s* At%	O*1s* At%
GO1h	67	33
GO2h	67	33
GO3h	66	34
GO5h	68	32

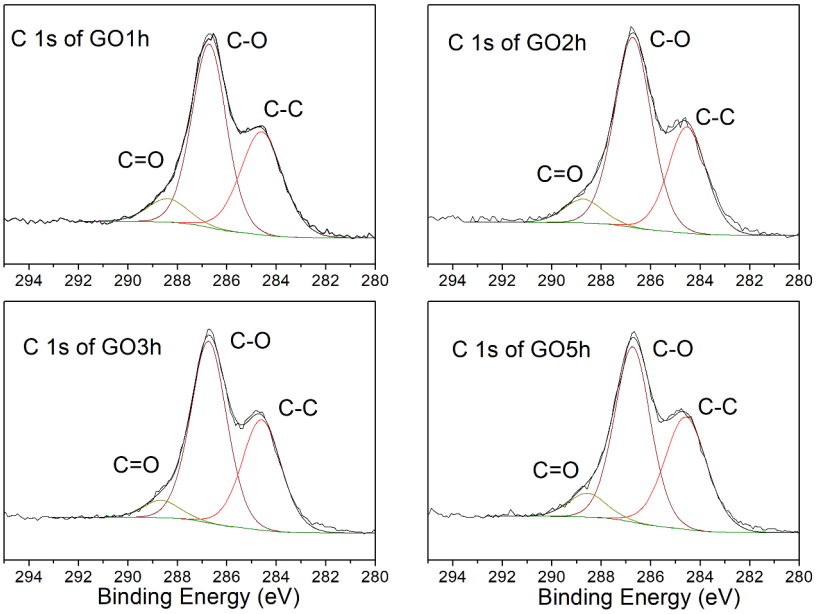

Figure 25: XPS C1s spectra of GO1h, GO2h, GO3h and GO5h

Table 13: Information of C1s bonds from XPS spectra of GO1h, GO2h, GO3h and GO5h

Codename	C-C Position (eV)	C-O Position (eV)	C=O Position (eV)	C-C At%	C-O At%	C=O At%
GO1h	284,6	286,72	288,4	38	54	8
GO2h	284,6	286,72	288,37	40	50	10
GO3h	284,6	286,74	288,51	37	53	10
GO5h	284,56	286,6	288,12	40	50	10

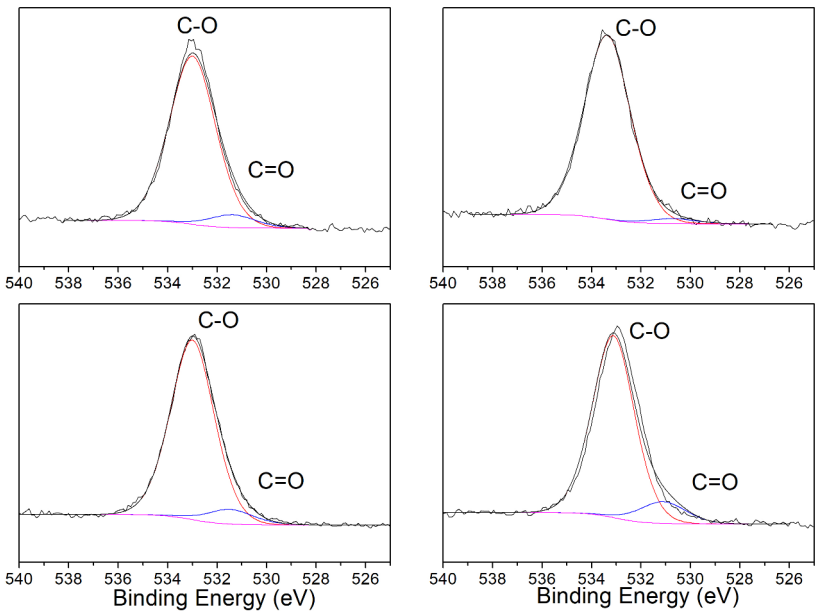

Figure 26: XPS O1s spectra of GO1h, GO2h, GO3h and GO5h

Table 14: Information of O1s bonds from XPS spectra of GO1h, GO2h, GO3h and GO5h

Codename	C=O Position (eV)	C-O Position (eV)	C=O At%	C-O At%
GO1h	531,4	533,0	7	93
GO2h	530,7	533,4	3	97
GO3h	531,5	533,0	8	92
GO5h	531,1	533,1	12	88

3.3.2

XPS spectra of GO2h and its RGO samples

In this section, XPS spectra of GO2h and RGO samples reduced from GO2h are analyzed. The samples tested are listed at table 15:

Table 15: List of GO2h and RGO samples reduced from GO2h for XPS characterization

Codename	Reduction temperature	Reduction time
GO2h	200ºC	0
RGO 200C 1h of GO2h	200ºC	1 hour
RGO 200C 2h of GO2h	200ºC	2 hours

From the XPS survey spectra of GO2h, RGO 200C 1h of GO2h and RGO 200C 2h of GO2h, we can find that after reduction, the carbon content surpasses the oxygen content. Both RGO 200C 1h of GO2h and RGO 200C 2h of GO2h correspond to an about 80% carbon content and an about 20% oxygen content. That means that after reduction GO lost more oxygen atoms. Further more, RGO 200C 2h of GO2h even has a little more carbon content and less oxygen content than RGO 200C 1h of GO2h does. That also indicates more oxygen was lost after more reduction time.

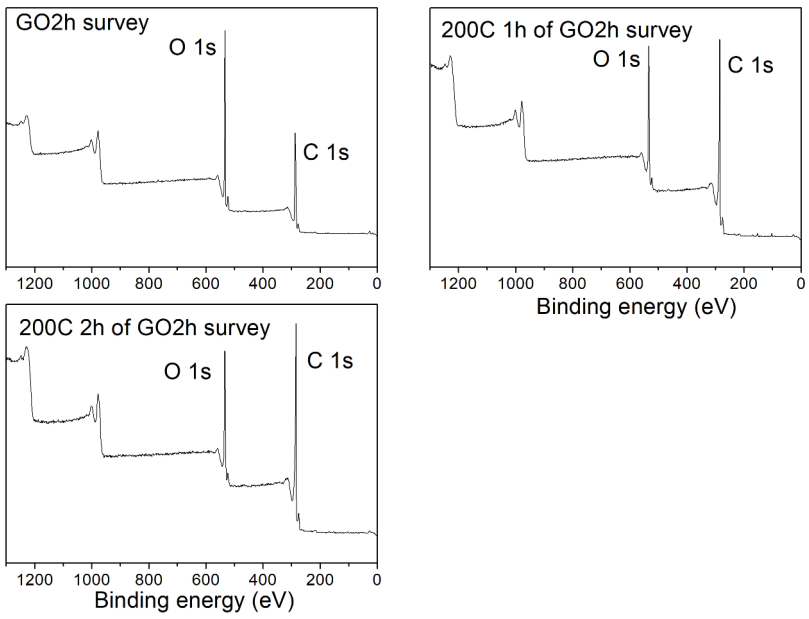

Figure 27: XPS survey spectra of GO2h and its RGO 200C 1h of GO2h and RGO 200C 2h of GO2h

Table 16: Information of XPS survey spectra of GO2h and its RGO 200C 1h of GO2h and RGO 200C 2h of GO2h

	C*1s* At%	O*1s* At%
GO2h	67	33
RGO 200C 1h of GO2h	80	20
RGO 200C 2h of GO2h	80	20

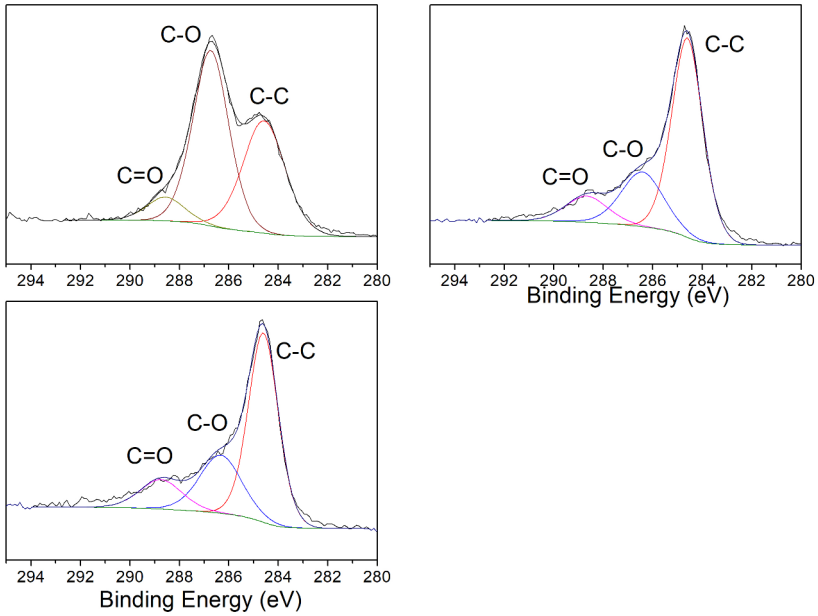

Figure 28: XPS C1s spectra of GO2h and its RGO 200C 1h of GO2h and RGO 200C 2h of GO2h

Table 17: Information of C1s bonds from XPS spectra of GO2h and its RGO 200C 1h of GO2h and RGO 200C 2h of GO2h

Codename	C-C Position (eV)	C-O Position (eV)	C=O Position (eV)	C-C At %	C-O At %	C=O At %
GO2h	284,6	286,7	288,4	40	50	10
RGO 200C 1h of GO2h	284,6	286,4	288,7	65	24	12
RGO 200C 2h of GO2h	284,6	286,3	288,8	60	26	13

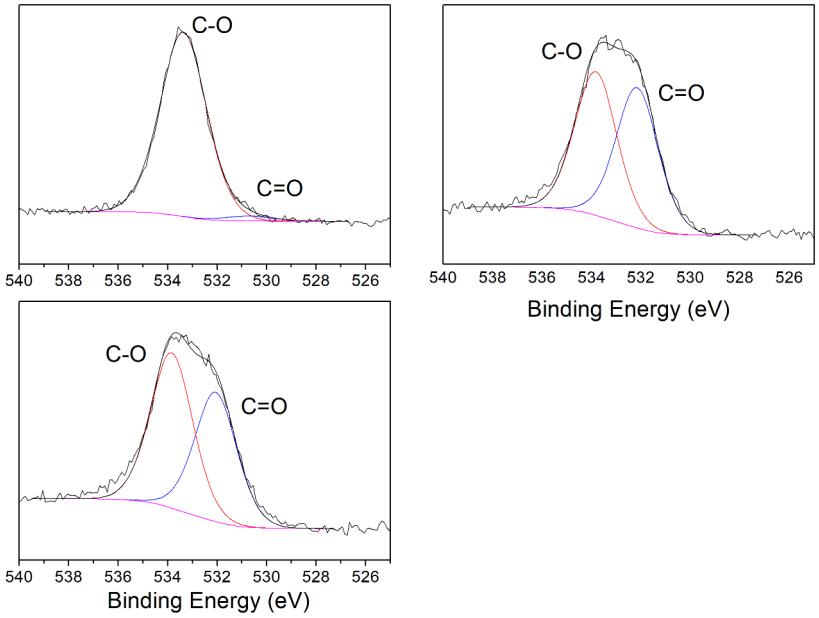

Figure 29: XPS O1s spectra of GO2h and its RGO 200C 1h of GO2h and RGO 200C 2h of GO2h

Table 18: Information of O1s bonds from XPS spectra of GO2h and its RGO 200C 1h of GO2h and RGO 200C 2h of GO2h

Codename	C=O Position (eV)	C-O Position (eV)	C=O At%	C-O At%
GO2h	530,7	533,4	3	97
RGO 200C 1h of GO2h	532,2	533,8	49	51
RGO 200C 2h of GO2h	532,1	533,8	45	55

4
Results of membranes

This chpter introduces results of membranes' performance. Flux and salt rejection are two factors of performance and tested for every membrane in experiment. First vacuum driving membranes of GO and RGO are tested. Then pure cellulose acetate PI membranes with different fabrication variants are tested and the membrane with excellent salt rejection (97%) is found. In the end, based on the best salt rejection membrane's recipe, CA-GO and CA-RGO PI membranes are tested.

4.1
Results of vacuum driving membranes

Vacuum driving membranes as mentioned in chapter 2.2 is a simple way to fabricate GO membranes. Herein, GO1D are used to make vacuum driving membranes. It's made of graphite flakes with a certain oxidation time, one day which is the reason why the sample code "GO1D" has "1D". Then, make a dense GO distilled water solution. Thus, we can take a certain volume of GO suspension to get a certain mass of GO. Next, dilute the GO suspension into distilled water. Finally, through filtering the dilute GO suspension with 0.22 μm nylon 6 filter and vacuum driving system, a GO membrane with a certain amount of GO is obtained.

0.1mg, 0.3mg, 0.5mg, 0.7mg, 1mg and 2.5mg GO1D are used to make vacuum driving membranes and later on the membranes are tested. Before testing, GO1D vacuum driving membranes are put into oven at 60ºC for one hour to dry itself and then are covered by permeable medical tape to prevent membranes from peeling off during testing. The feed solution is NaCl solution, and its concentration is 4000 ppm. The pump's working pressure is 10 bar. Their performances are shown below:

Table 19: Performance of GO1D vacuum driving membranes

GO1D	Flux (LMH)	Rejection
0.1mg	870.3	0%
0.3mg	27.2	0%
0.5mg	19.9	3%
0.7mg	5.3	25%
1mg	5.3	25%
2.5mg	2.1	61%

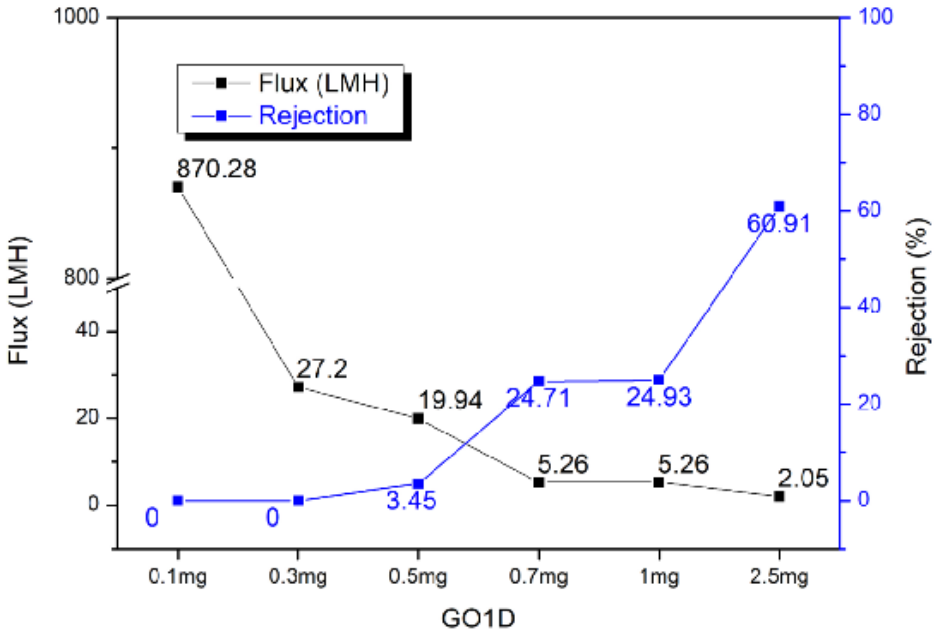

From the table 19, we can find that 0.1mg and 0.3mg GO1D membranes show a large flux and 0% rejection. The reason is probably that 0.1mg and 0.3mg GO1D is not enough to cover the filter. Along with GO1D increasing, membranes' rejection increases as well. Especially, 2.5mg GO1D membrane shows a 60.91% rejection. However, membranes' permeability decreases quickly along with increasing of GO accumulation. Decreasing of flux also reflects on its fabrication process: it takes more than 10 hours to fabricate the 2.5mg membrane, and it only takes less than one hour to fabricate the other GO1D membranes with less than

1mg. For filters with same area, GO's accumulation increases path for water molecule and possibility that salt ions are adsorpted on the GO capillary maze. So permeance flux gets smaller and salt rejection gets better along with GO's increasing.

Next, 0.5mg GO1D membranes are reduced by oven at 200ºC for 1, 2 and 3 hours. Performances of these RGO membranes is recorded at table 20:

Table 20: Performances of RGO 200ºC of GO1D vacuum driving membranes

GO1D	Reduce time	Flux (LMH)	Rejection
0.5mg	1h	2,4	7%
0.5mg	2h	0,9	44%
0.5mg	3h	2,1	15%

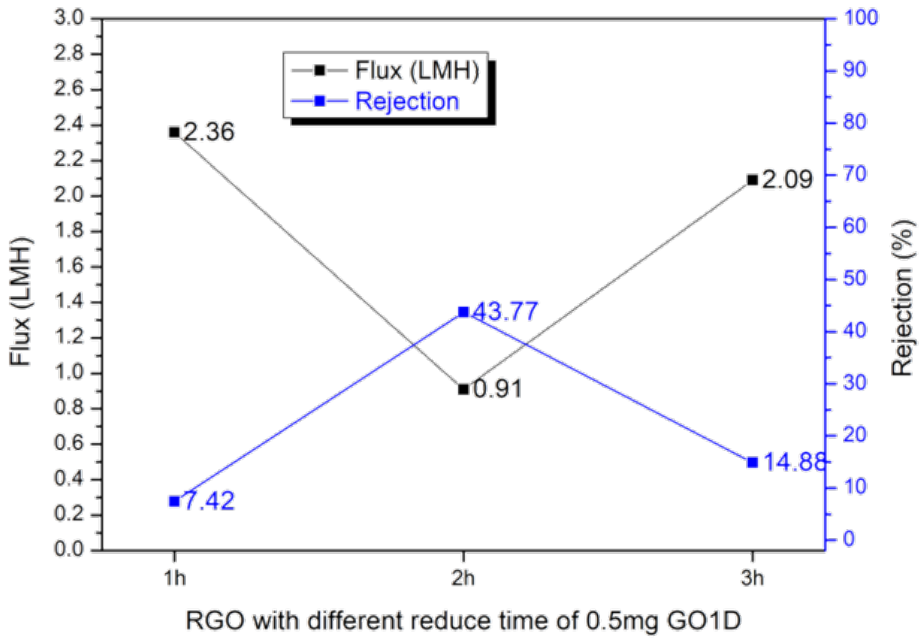

Even though 2h 0.5mg RGO has a better rejection than 3h 0.5mg RGO, both 2h 0.5mg RGO and 3h 0.5mg RGO have better rejection and worse flux compared with 1h 0.5mg RGO. After reduction process, distance between GO laminates decreases, which increases membrane's salt rejection ability. Abnormal result

between 2h and 3h RGO is caused by defects that can be formed during manufacturing or reduction processes. And all three 0.5mg RGO have a better rejection of 0.5mg GO membrane. That means reduction treatment increases GO membrane's rejection. As for 1mg RGO, its permeance flux is too small to measure its product water volume and its salt rejection. 2.5mg RGO's permeance flux is 0.

4.2
Results of phase inversion membranes

Cellulose acetate (CA) membranes are made by phase inversion (PI) method. The method is described in a previous chapter, the steps in short are:

1. Make the CA solution, in another word, dissolve CA into acetone and DMF, and stir the system with magnetic bar until homogeneous.

2. Cast the solution on glass plate with doctor blade in a specific height. Evaporate the casted solution for a certain time.

3. Immerse the glass plate with the casted solution into ice water bath for one hour.

4. Take the membrane out from the ice water bath, and immerse it into hot water bath in a certain temperature for a certain time.

According to the membrane forming mechanism mentioned before, we can explore CA membrane's permeability and salt rejection through controlling the following factors:

1. Cellulose acetate's content.

As membrane's skeleton, CA definitely makes a big influence to membrane's properties.

2. Ratio of acetone to DMF.

Acetone and DMF are solution's solvents. After that the solution is casted on the glass plate, volatile solvent evaporates and lefts a dense layer solution that is the

original state of selective layer. Acetone is much more volatile than DMF. The difference of volatility offers an opportunity to control the forming of rejection ability via changing the ratio of acetone to DMF.

3. Membrane's thickness.

Membrane's thickness is adjusted by changing the height of doctor blade. However, after the whole fabrication process, the membrane's thickness will be shrinked, because during the evaporation and immersion, solvent is lost. Therefore, the actual thickness is always thinner than doctor blade's height. Membrane's thickness doesn't influence membranes' rejection.

4. Evaporation time.

Membranes' selective layer is formed during evaporation process. Controlling evaporation time is a main way to tuning membranes' pore size.

5. Post treatment

Hot water bath is used as post treatment. This step is very one of the most important steps to achieve membranes' final salt rejection ability, another one is evaporation time. Herein, hot water bath temperature and hot water bath time are two factors to control this process.

Besides, the room temperature and humidity in laboratory also have possibility to influence the performance of membrane. Considering the reality, it's difficult to keep the laboratory under a certain temperature and humidity. But I tried to keep the temperature is around 22-23ºC and relative humidity is about 40-60%.

In the rest of this section, the influence of these factors will be explored one by one.

4.2.1

Cellulose acetate's content

Cellulose acetate is membrane's core material. It forms membrane's main structure. In order to research cellulose acetate content influence, the volume of acetone is fixed as 2 mL and the volumes of DMF are 1.065 mL, 1.05 mL, 1.04 mL, 1.02 mL and 1.05 mL respectively. As for cellulose acetate content, 0.257g, 0.367g, 0.490g,0.540g and 0.600g CA are adopted, and they take 10%, 12.5%,

15%, 17.5% and 19.0% of total mass of solutions. The data is organized in the following table.

Table 21: Samples with different cellulose acetate content

Codename	Mass of CA	Percentage of CA	Volume of Acetone	Volume of DMF
CA10	0.257g	10,0%	2 mL	1.065 mL
CA12.5	0.397g	12,5%	2 mL	1.05 mL
CA15	0.490g	15,0%	2 mL	1.04 mL
CA17.5	0.540g	17,5%	2 mL	1.02 mL
CA19.0	0.600g	19,0%	2 mL	1.05 mL

Other conditions are kept in same: doctor blade's height is set as 100 μm; evaporation time is 30 seconds and post treatment is not adopted.

Table 22: Performance of membranes with different CA content

Codename	Flux (LMH)	Rejection (%)
CA10	31396.4	0%
CA12.5	361.1	2%
CA15	193.6	0%
CA17.5	109.9	5%
CA19.0	23.5	30%

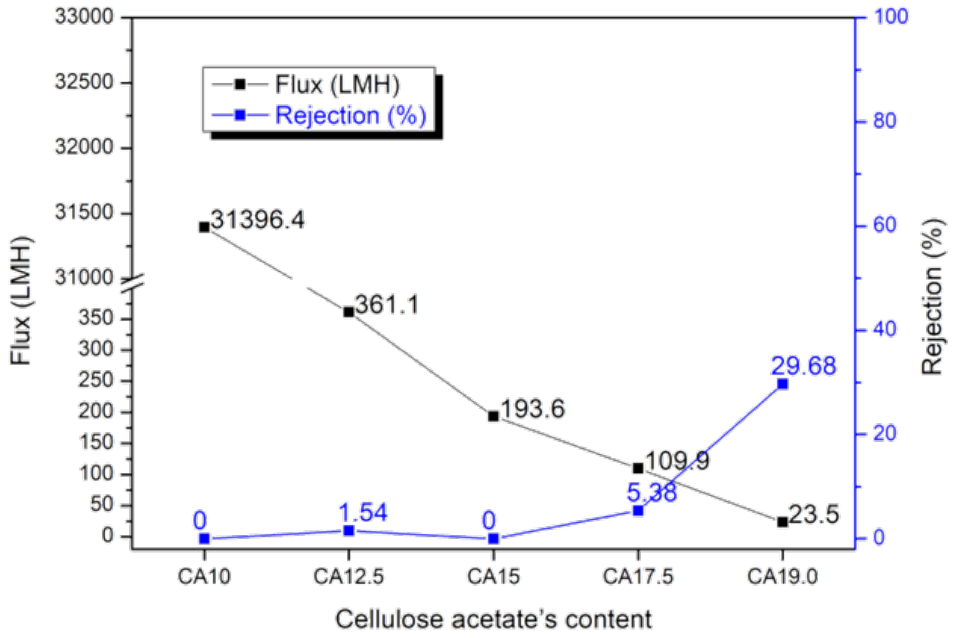

From the result, we can see that flux is getting smaller and membrane's rejection is becoming higher along with CA content's increase. CA10 shows an extreme huge flux and 0 rejection. That may mean a loose structure creates big pores. CA19.0 demonstrates a relatively good rejection and the smallest flux among these 5 membranes. Its good rejection should credit to its denser structure. CA12.5 shows a very big flux and an ability of salt rejection. Big flux is convenient to test and compare and its limited ability of rejection has a big potential to improve. Therefore, CA12.5 is used as a reference for the following experiments.

4.2.2

Ratio of acetone to DMF

In order to explore the influence of ratio of acetone to DMF in membrane, 5 samples are prepared. As mentioned in last paragraph, CA12.5 is used as a reference. So, the CA content in the 5 samples is 12.5%. Then, the total mass of acetone and DMF is fixed, which is 77.5%. The solvent part, 77.5% of total mass, is divided into 5 different ratios of acetone to DMF, which are 0:1, 1:3, 1:1, 3:1 and 1:0. 0:1means DMF occupies 100% of the solvent part; 1:3 means that

acetone takes 25% of the solvent part and DMF takes 75%; 1:1 means both acetone and DMF takes 50% of the solvent part; 3:1 means acetone takes 75% and DMF takes 25%; 1:0 means that acetone takes all the share of the solvent part.

Table 23: Samples of different ratio of acetone to DMF

Codename	Ratio	Acetone		DMF	
		Percentage	Volume	Percentage	Volume
R1	0:1	0%	0mL	100%	2.21mL
R2	1:3	25%	0.665mL	75%	1.658mL
R3	1:1	50%	1.329mL	50%	1.105mL
R4	3:1	75%	1.994mL	25%	0.553mL
R5	1:0	100%	2.658mL	0%	0mL

Herein, CA is 0.3g and takes 12.5% of the total mass. Doctor blade's height is set as 200 μm; evaporation time is 30 seconds and post treatment is not adopted.

Table 24: Performance of membranes with different ratio of acetone to DMF

Codename	Flux (LMH)	Rejection (%)
R1	941,9	1%
R2	1007,3	2%
R3	17,8	9%
R4	0,8	0%
R5	87,7	1%

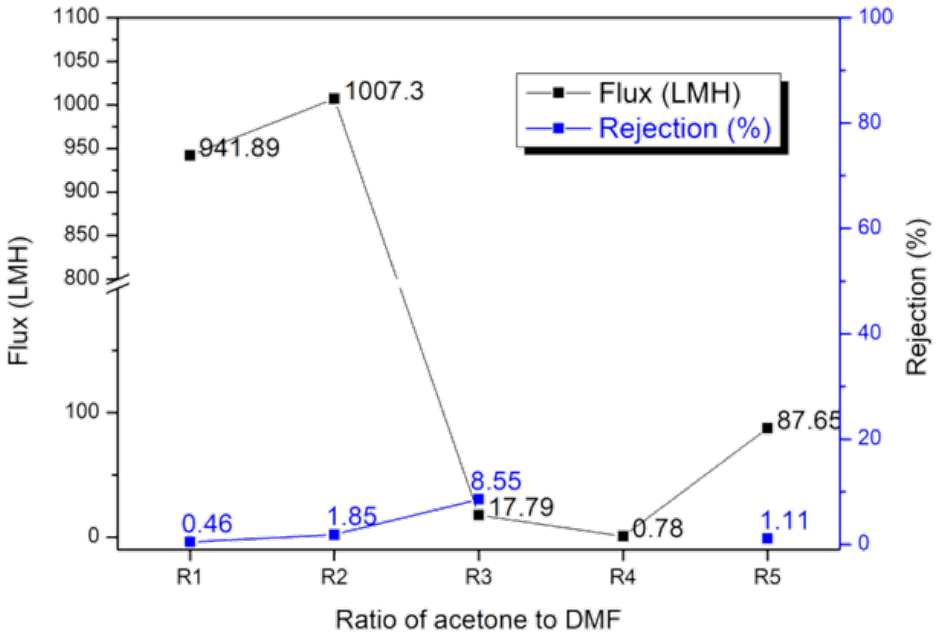

According the results, both more acetone and more DMF make membranes have a better flux. When acetone dominates the solvent part of the CA solution due to the strong volatility of acetone, more and larger pores were formed during the evaporation process. These big pores enlarge the membranes' flux and worsen their salt rejection at the same time. When DMF dominates the solvent part of the CA solution, the casted solution on the glass plate didn't loose volatile gas from itself. Therefore, concentration of the solution's surface didn't change and CA remains its loose structure which leads to a big flux too. So R1, R2 and R5's rejection is worse than the middle samples. By the way, R4 doesn't have its rejection result, because the volume of product water is not enough to measure its conductivity. In summary, too much acetone or DMF damage membranes' flux and rejection. Trying to make the ratio of acetone to DMF between R2 and R4 is a good choice.

4.2.3

Membrane's thickness

Membrane's thickness is not determined by only doctor blade's height, but also the fabrication process. After casting the solution, volatile gas evaporates from the

solution and reduces the membrane's thickness. In post treatment, hot water shrinks the membrane's size, including its thickness. Below are 5 samples with different thickness:

Table 25: Comparison of doctor blade height and actual thickness

Codename	Doctor blade height	Actual thickness
CA12.5	100 μm	50 μm
T2	150 μm	90 μm
T3	200 μm	80-100 μm
T4	250 μm	180 μm
T5	300 μm	200 μm

These 5 membranes share the same solution with CA12.5 membrane. Evaporation time is 30 seconds and post treatment is not adopted.

The smallest unit on the doctor blade is 20 μm. So, the thinnest membrane that can be made by this PI system is about 20 μm. However, thin membranes are more fragile, it's easy to get destroyed during the fabrication process. What's more, if considering doping other material into the solution, just like GO or RGO, thin membrane's unit area will contain less materials than thicker ones.

Some studies found that the thicker the membrane, the more macrovoids are formed.(54) Air bubbles often hide in the front of the casting solution. Along with the casting process, bubbles are covered by the membrane. If the membrane is thin enough, bubbles will get out the membrane easily without damages. If the membrane is too thick, bubbles will get stuck in the membrane, lefting a hollow. Besides, evaporation also creates many bubbles. Because of the same mechanism, thick membranes are easier to get destroyed by the bubbles.

These 5 membranes' performance is at table 26:

Table 26: Performance of membranes with different thickness

	Flux (LMH)	Rejection
CA12.5	361,1	2%
T2	143,9	2%

T3	12,8	5%
T4	6,0	13%
T5	8,4	9%

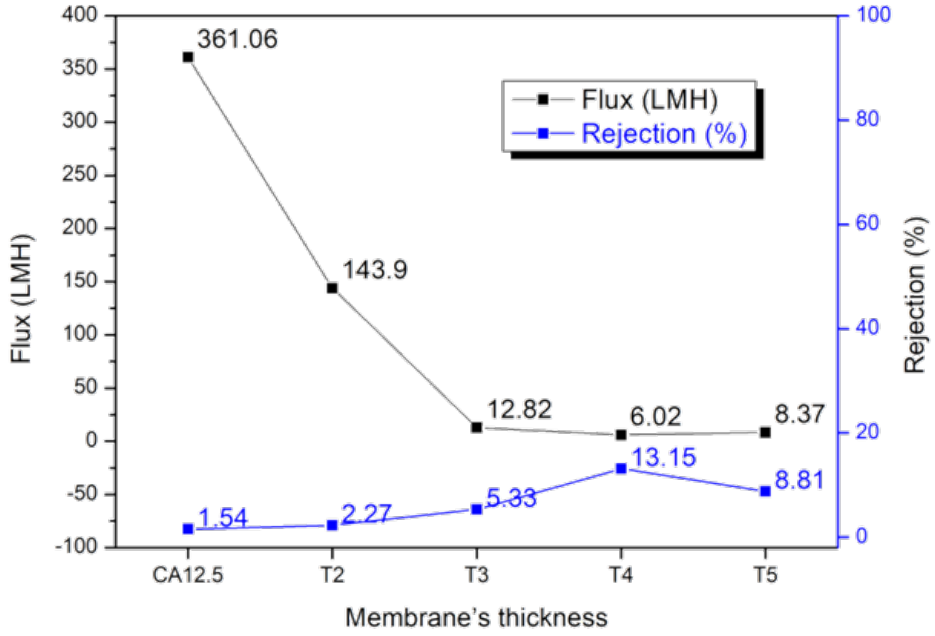

According to the performance of membranes with different thickness, we find that thinner membranes have a huge flux and a worse salt rejection. Thick membranes are the opposite. But in experiments, both very thin and very thick membranes have a high possibility to be destroyed during fabrication process or testing. Considering the performance and the durability, 200 μm doctor blade height is adopted to be a default thickness, which is also 80-100 μm actual thickness of membranes.

4.2.4

Evaporation time

Evaporation step is commonly used to obtain less porous membrane surfaces when volatile solvent is present in the casting solution.(55) Evaporation is the key step of forming the selective layer, which makes volatile solution away from the cast solution. However, finding the best evaporation time is not easy. Here the best evaporation time means the membrane formed in this evaporation time has its best

salt rejection. According to my research, there is not a general best evaporation time that benefits different membranes. In fact, different membranes have their own best evaporation time. It's easy to understand, because different content of CA or different ratio of acetone to DMF influence the membranes structures or evaporation. However, environment also plays an important role in membranes formation. It is obvious that the higher temperature, the more volatile solvent will evaporate.(56) Relative humidity is another important parameter in the membrane synthesis process. But it is not easy to investigate in a lab-scale the role of the atmosphere.(57) If the synthesis is processing at relatively high humidity level, water could condense on the membrane and locally lower the temperature of the cast film.(58) Therefore, the lab's atmosphere is kept at around 22-23ºC and 40-60% relative humidity.

Let's use CA12.5 (CA 0.397g, acetone 2 mL and DMF 1.05 mL) as the first sample to explore its best evaporation time. The rest synthesis conditions are 200 μm doctor blade height, 22-23ºC and about 50% relative humidity without post treatment. Ten membranes were fabricated under same recipe except the evaporation time. The evaporation times are integer minutes and alters from 1 minute to 10 minutes. Table 27 is the performance of these ten membranes with different evaporation time:

Table 27: Performance of CA12.5 with different evaporation time

	Evaporation time	Flux (LMH)	Rejection
E1	1 min	116,0	5%
E2	2 min	31,7	5%
E3	3 min	38,1	6%
E4	4 min	58,0	3%
E5	5 min	16,3	43%
E6	6 min	15,4	39%
E7	7 min	30,8	21%
E8	8 min	83,4	1%
E9	9 min	197,6	0%
E10	10 min	656,3	3%

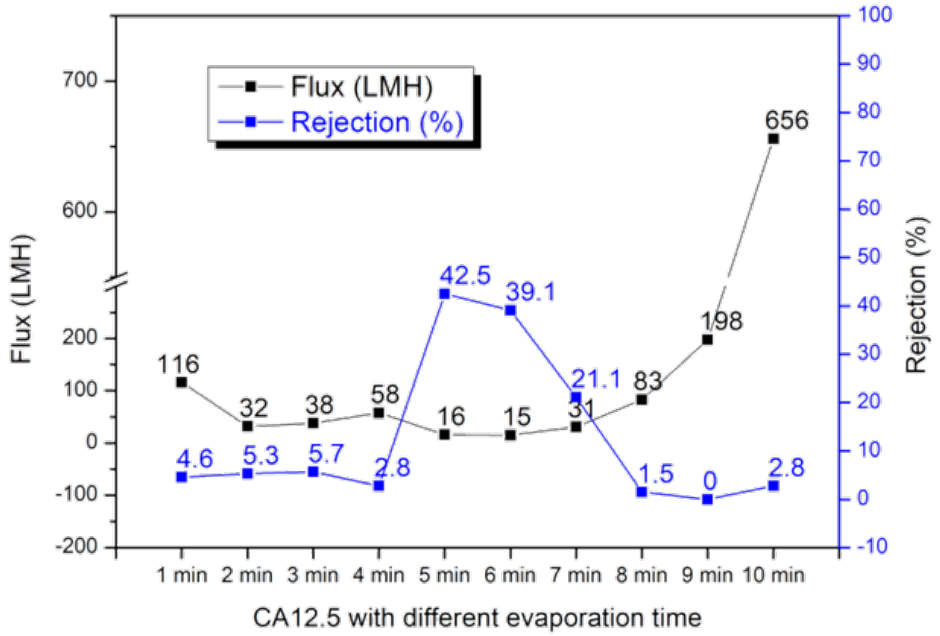

From performance's table, we can find that the permeate gets smaller along the increase of evaporation time. And its flux becomes smallest when evaporation time is 5 or 6 minutes. On the other side, rejection' performance is the opposite. Rejection ability increases from 1 min evaporation, and gets its best in 5-6 min evaporation time. Along with the evaporation time extending, membranes' rejection becomes worse and worse. From the results, CA12.5's best evaporation time is around 5 min.

Through controlling evaporation time, CA12.5's performance gets a big improvement, especially at its own best evaporation time. In section "Cellulose acetate's content", CA12.5's rejection is not the best one, but CA19.0 shows the best salt rejection compared with other samples. Can CA19.0's rejection ability be improved further through controlling the evaporation time? Below is CA19.0's performance in different evaporation time:

Table 28: Performance of CA19.0 with different evaporation time

	Evaporation time	Flux (LMH)	Rejection
V1	0s	32,6	1%
V2	30s	1,5	7%

V3	40s	1,6	26%
V4	50s	1,6	22%
V5	60s	2,7	61%
V6	70s	7,7	24%
V7	90s	13,1	10%
V8	120s	20,9	6%
V9	300s	598,3	1%

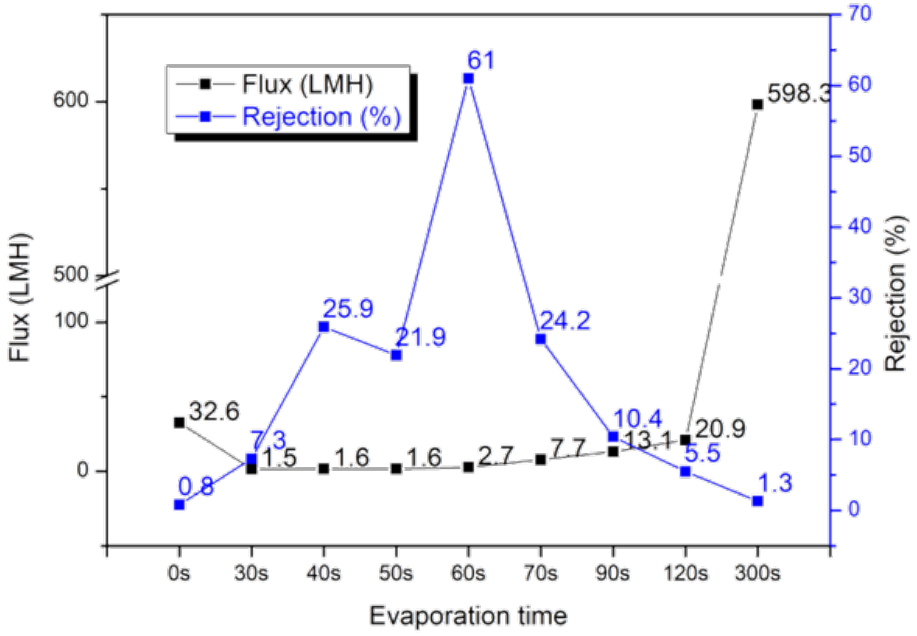

According CA19.0's results, 1 minute should be CA19.0's best evaporation time. This time is different from CA12.5's, indicating different solution with different best evaporation time. Evaporation time longer or shorter than the best evaporation time make membrane's flux larger and reduce membrane's rejection. Shorter evaporation means selective layer is not formed completely, and the remained structure doesn't offer good rejection. In contrast, after a long evaporation, the pores in selective layer are enlarged by excessive volatile gas.

Different solution has different contents of every component, which can influence the evaporation of volatile solvent. Therefore, different solution has their own best evaporation time.

Evaporation time is indeed a key factor to control membrane's flux and rejection. Through adjusting evaporation time, salt rejection performance of CA12.5 and CA19.0 get improved, but the rejection is still far away from practical rejection percentage, at least 90%.

4.2.5
Post treatment

Post treatment is the final and a very important process of synthesis PI membrane. Post treatment can increase CA membrane's salt rejection significantly, but decreases membrane's permeability. Besides, post treatment also increase CA membrane's durability.(58) For CA membrane, hot water bath treatment is a very common way to improve its performance. In this section, temperature and time of hot water bath treatment are two factors needed to be explored.

CA19.0 is adopted as tested membrane in following content. CA19.0 solution is made of 0.6 g cellulose acetate, 2 mL acetone and 1.05 mL DMF. CA19.0 solution is casted by 200 μm height doctor blade. Evaporation time is 1 minute.

After the synthesis process mentioned in last paragraph is completed, the membrane should be treated by hot water bath. First, bath time is explored, here CA19.0 membrane is treated by 60ºC:

Table 29: Performance of CA19.0 with different bath treatment time under 60ºC

Post treatment time	Flux (LMH)	Rejection
1 min	2,4	54%
3 min	3,5	71%
5 min	5,0	57%
8 min	2,4	49%
10 min	1,3	68%
15 min	1,8	36%

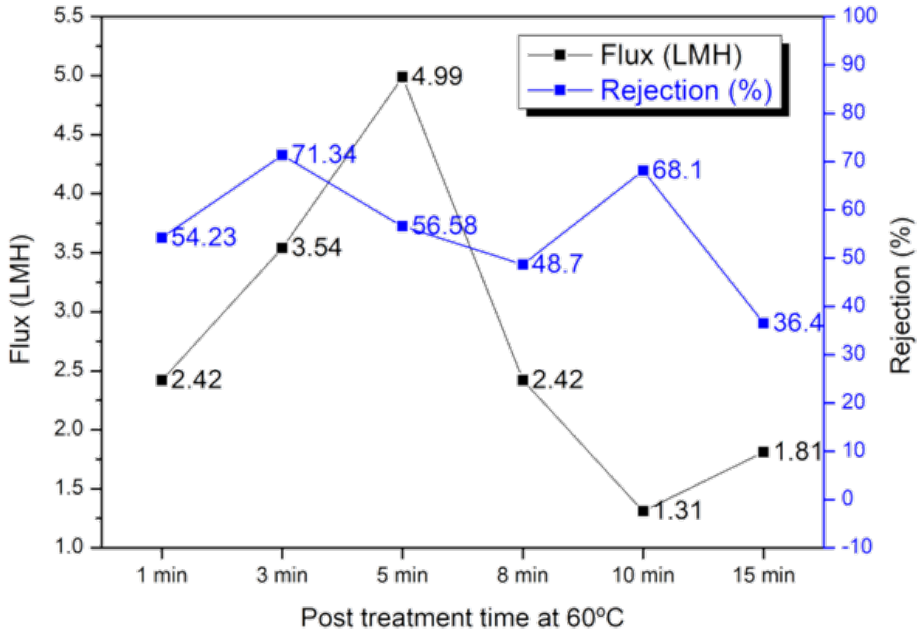

From the table, we can find that CA membranes that experienced post treatment show a better rejection ability than those without hot bath treatment. However, the flux decreases significantly. Both flux and rejection don't have a clear relation with post treatment time increasing. This situation may be caused by uneven heating of hot plate in operation. 60ºC isn't a high temperature, but membranes get a better rejection than before. Next, for achieving better rejection, hotter temperature bath is needed. Therefore, 70, 80 and 90ºC are introduced into the hot bath treatment, and the treatment time is fixed as 10 minutes.

Table 30: Performance of CA19.0 with different temperature in post treatment

Temperature (ºC)	Flux (LMH)	Rejection
60	1,3	68%
70	3,2	44%
80	2,0	68%
90	1,1	97%

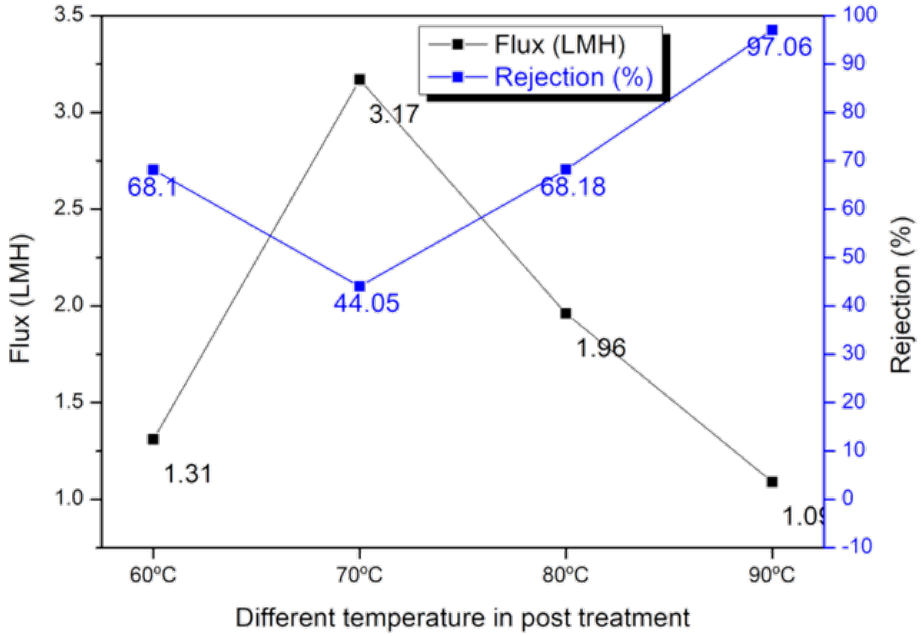

Hotter water bath treatment increases membranes' rejection significantly. In particular, 90 degree water bath treatment achieves 97.06% rejection. At the same time, membranes' permeability is reduced.

In summary, CA's content, ratio of acetone to DMF, membrane's thickness, evaporation time and post treatment, as five factors influencing the performance of membranes, are tested and their properties of improving salt rejection are added together. Finally, a membrane with 97.06% rejection is achieved, although its flux is very small.

4.2.6

CA-GO and CA-RGO membranes

As shown in last section, CA membranes with high salt rejection are found. Based on this result, through 5 factors' investigation. Based on this result, GO and RGO are introduced to fabricate CA-GO and CA-RGO membranes. GO and RGO's properties as desalination materials are shown in chapter 3.2. And both GO and RGO show their potential in salt rejection. Therefore, CA-GO and CA-RGO membranes have an attraction to explore.

For CA-GO membranes, 30mg GO1D is adopted and CA19.0 is also used. Other materials and fabrication process are same as CA19.0 membrane. First, dissolve 10mg GO into 6 mL acetone and 3.15 mL DMF solution. Utilize ultrasonic cleaning machine exfoliate the GO in solvents for about 3 hours until GO dissolving into the solvents homogeneously. Here is a small tip: shake the bottle holding GO suspension, if there is not any obvious GO stack attached on the bottle's inner wall, that means GO dissolved and huge GO stack is exfoliated. Then, 1.8 g cellulose acetate is added into the GO suspension. After stirring for overnight, the CA-GO suspension is obtained. Next CA-GO suspension is casted by 200 μm height doctor blade with evaporation time of 1 minute. And the prepared membranes were subjected a post treatment for 10 minutes in 90ºC water bath.

As for CA-RGO membrane, its preparation process is the same as CA-GO's. The only difference is that replacing the 30 mg GO with 30 mg RGO. The RGO used here is made from GO1D. And GO1D is reduced at 200ºC for one hour.

The performances of CA-GO and CA-RGO membranes are shown as below:

Table 31: Performances of CA-GO and CA-RGO membranes

	Flux (LMH)	Rejection
CA19.0	1,1	97%
CA-30mg GO	0,8	51%
CA-30mg RGO	0,6	69%

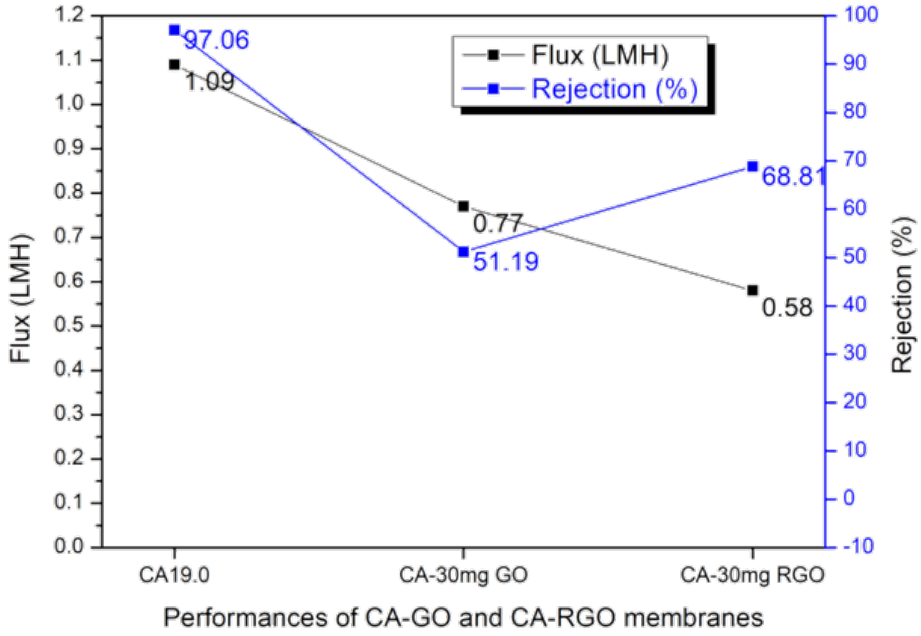

According its result, after doping GO or RGO into the CA membrane, both flux and rejection are worsened.

There are three possible speculations why rejection gets worse in CA-GO and CA-RGO membranes:

CA membrane's structure contains selective layer and support layer. Selective layer is more dense and contains smaller pores which is slightly smaller than the size of hydrated ions, about 0.7 nm. And support layer contains big pores which are much larger than hydrated ions and macrovoid which is in micron scale. Due to GO and RGO vacuum driving membranes' rejection performance, the average distance between GO or RGO laminates is slightly larger than hydrated ions.

After CA membrane's structure is mixed with GO or RGO powder, both its selective layer and support layer are influenced. In selective layer, interface between the GO or RGO and CA structure has larger pores, which worsen the salt rejection in CA-GO or CA-RGO membranes. In support layer, GO and RGO platelets block the big pores, which leads a smaller flux in both GO-CA and RGO-CA membranes. As for the comparison of GO-CA and RGO-CA, the results of GO and RGO vacuum driving membranes can explain.

5
Perspective

In this work, vacuum driving membranes and phase reversion membranes are introduced. Based on these two methods, GO vacuum membranes, RGO vacuum membranes, CA membranes, CA-GO membranes and CA-RGO membranes are made to explore the possibility as reverse osmosis membrane.

For GO vacuum driving membranes and RGO vacuum membranes, the selective layer for water-ion separation is pure GO or RGO. GO1D and RGO reduced from GO1D vacuum driving membranes show their limited salt rejection potential. For example, 2.5 mg GO1D vacuum membrane has 2.05 LMH flux and 61% rejection. However, along with inscreasing GO's mass, its flux drops to zero quickly. As for RGO vacuum driving membranes, nylon 6 filter always deform in high temperature during the reduction process. It is a challenge to prevent the RGO vacuum membranes, especially the RGO layer, from being destroyed after reduction.

For pure cellulose acetate membranes, five major factors are chosen to investigate their influence to flux and salt rejection. The five factors are: CA's content, ratio of acetone to DMF, membrane's thickness, evaporation time and post treatment.

1. CA' content

More CA's content means less flux and better salt rejection.

2. Ratio of acetone to DMF

Both more acetone and more DMF in the solution mean bigger flux and worse salt rejection.

3. Membrane's thickness

Thicker membrane improves slight rejection, but decrease a lot of flux. Besides, both very thick (more than 250 μm) and very thin (less than 40 μm) make membranes fragile.

4. Evaporation time

Solution with different contents of cellulose acetate, acetone and DMF has different best evaporation time. Both longer and shorter evaporation time lead to larger flux and worse salt rejection.

5. Post treatment

Higher temperature or longer post treatment time will make membranes a smaller flux and better salt rejection. But too long post treatment time can also make membranes impermeable.

After exploring the 5 factors, a membrane with codename CA19.0 is found with 97% salt rejection and 1.1 LMH flux. Then, CA19.0 was used to mix with GO and RGO to make GO-CA and RGO-CA membranes, which show their rejection ability worse than CA19.0.

In the future work, exploring the limit of performance of GO and RGO is the key. It is still not clear if GO or RGO will be revolutionary material for desalination. But their performance's limit in vacuum driving membrane and CA phase inversion membrane can be worked out at least. And which type of oxygen functional groups are attached or detached during oxidation or reduction is worth to investigate.

References

1. Lee KP, Arnot TC, Mattia D. A review of RO membrane materials for desalination-Development to date and future potential. J Memb Sci [Internet]. 2011;370(1–2):1–22. Available from: http://dx.doi.org/10.1016/j.memsci.2010.12.036

2. Rodríguez-Calvo A, Silva-Castro GA, Osorio F, González-López J, Calvo C. RO seawater desalination: current status of membrane systems. Desalin Water Treat [Internet]. 2015;56(4):849–61. Available from: http://dx.doi.org/10.1080/19443994.2014.942378

3. Johnson DJ, Hilal N. Can graphene and graphene oxide materials revolutionise desalination processes? Vol. 500, Desalination. 2021.

4. Shiklomanov I a. World Water Resources. A new appraisal and assessment for the 21st century. United Nations Educational, Scientific and Cultural Organization. 1998. p. 40.

5. WHO/UNICEF. Five years into the SDGs progress on household drinking water, sanitation and hygiene WHO/UNICEF joint monitoring programme for water supply, sanitation and hygiene [Internet]. Joint Water Supply, & Sanitation Monitoring Programme. 2021. Available from: http://apps.who.int/bookorders.

6. Salameh MTB, Alraggad M, Harahsheh ST. The water crisis and the conflict in the Middle East. Vol. 7, Sustainable Water Resources Management. 2021.

7. Moreira F de S, Lopes MPC, de Freitas MAV, Antunes AM de S. Future scenarios for the development of the desalination industry in contexts of water scarcity: A Brazilian case study. Technol Forecast Soc Change. 2021;167.

8. Ahmed FE, Khalil A, Hilal N. Emerging desalination technologies: Current status, challenges and future trends. Vol. 517, Desalination. 2021.

9. Chen JP, Wang LK, Yang L, Zheng Y-M. Desalination of Seawater by Thermal Distillation and Electrodialysis Technologies. Membrane and Desalination Technologies. 2011. p. 525–58.

10. Lee KP, Arnot TC, Mattia D. A review of RO membrane materials for desalination-Development to date and future potential. J Memb Sci. 2011;370(1–2):1–22.

11. McGinnis RL, Elimelech M. Energy requirements of ammonia-carbon dioxide forward osmosis desalination. Desalination. 2007;207(1–3):370–82.

12. Goh PS, Lau WJ, Othman MHD, Ismail AF. Membrane fouling in desalination and its mitigation strategies. Desalination. 2018;425(October 2017):130–55.

13. Reid CE, Breton EJ. Water and ion flow across cellulosic membranes. Vol. 1, Journal of Applied Polymer Science. 1959. p. 133–43.

14. S. Loeb SS. Sea Water Demineralization by Means of an Osmotic Membrane. Saline Water Convers - II SeaSociety, Am Chem [Internet]. 1963;38:117–32. Available from: http://pubs.acs.org/doi/book/10.1021/ba-1963-0038

15. Cadotte JE, Petersen RJ, Larson RE, Erickson EE. A new thin-film composite seawater RO membrane. Desalination. 1980;32(C):25–31.

16. Freger V, Ramon GZ. Polyamide desalination membranes: Formation, structure, and properties. Vol. 122, Progress in Polymer Science. 2021.

17. K. S. Novoselov, A. K. Geim, S. V. Morozov, D. Jiang, Y. Zhang, S. V. Dubonos IVG and AAF. Electric Field Effect in Atomically Thin Carbon Films. Vol. 306. 2016. p. 666–9.

18. Cao Y, Fatemi V, Fang S, Watanabe K, Taniguchi T, Kaxiras E, et al. Unconventional superconductivity in magic-angle graphene superlattices. Vol. 556, Nature. 2018. p. 43–50.

19. Cao K, Feng S, Han Y, Gao L, Hue Ly T, Xu Z, et al. Elastic straining of free-standing monolayer graphene. Vol. 11, Nature Communications. 2020.

20. Surwade SP, Smirnov SN, Vlassiouk I V., Unocic RR, Veith GM, Dai S, et al. Water desalination using nanoporous single-layer graphene. Nat Nanotechnol [Internet]. 2015;10(5):459–64. Available from: http://dx.doi.org/10.1038/nnano.2015.37

21. Gao W. The chemistry of graphene oxide. Graphene Oxide Reduct Recipes, Spectrosc Appl. 2015;61–95.

22. Material SO, Press H, York N, Nw A. Unimpeded Permeation of Water. Science (80-) [Internet]. 2012;442(January):442–4. Available from: http://www.sciencemag.org/content/335/6067/442.abstract

23. Nair RR, Wu HA, Jayaram PN, Grigorieva I V., Geim AK. Unimpeded permeation of water through helium-leak-tight graphene-based membranes. Science (80-). 2012;335(6067):442–4.

24. Sun P, Wang K, Zhu H. Recent Developments in Graphene-Based Membranes: Structure, Mass-Transport Mechanism and Potential Applications. Adv Mater. 2016;28(12):2287–310.

25. Mi B. Graphene oxide membranes for ionic and molecular sieving. Science (80-). 2014;343(6172):740–2.

26. Abraham J, Vasu KS, Williams CD, Gopinadhan K, Su Y, Cherian CT, et al. Tunable sieving of ions using graphene oxide membranes. Nat Nanotechnol [Internet]. 2017;12(6):546–50. Available from: http://dx.doi.org/10.1038/nnano.2017.21

27. Boukhvalov DW, Katsnelson MI, Son YW. Origin of anomalous water permeation through graphene oxide membrane. Nano Lett. 2013;13(8):3930–5.

28. Thomson. On the atomic weight of barytes. Philos Mag. 1831;10(59):392–4.

29. Hummers, William S.; Offeman RE, Hummers Richard E. WS. O. Preparation of Graphitic Oxide [Internet]. Vol. 80, Journal of the American Chemical Society. 1958. p. 1937. Available from: https://pubs.acs.org/sharingguidelines

30. Yan P, Zhang B, Wu KH, Su D, Qi W. Surface chemistry of nanocarbon: Characterization strategies from the viewpoint of catalysis and energy conversion. Carbon N Y [Internet]. 2019;143:915–36. Available from: https://doi.org/10.1016/j.carbon.2018.11.085

31. Zhou JH, Sui ZJ, Zhu J, Li P, Chen D, Dai YC, et al. Characterization of surface oxygen complexes on carbon nanofibers by TPD, XPS and FT-IR. Carbon N Y. 2007;45(4):785–96.

32. Burg P, Fydrych P, Cagniant D, Nanse G, Bimer J, Jankowska A. The characterization of nitrogen-enriched activated carbons by IR, XPS and LSER methods. Carbon N Y [Internet]. 2002;40(9):1521–31. Available from: https://doi.org/10.1016/S0008-6223(02)00004-0

33. Martínez MT, Callejas MA, Benito AM, Cochet M, Seeger T, Ansón A, et al. Sensitivity of single wall carbon nanotubes to oxidative processing:

Structural modification, intercalation and functionalisation. Vol. 41, Carbon. 2003. p. 2247–56.

34. Anariba F, Viswanathan U, Bocian DF, McCreery RL. Determination of the structure and orientation of organic molecules tethered to flat graphitic carbon by ATR-FT-IR and Raman spectroscopy [Internet]. Vol. 78, Analytical Chemistry. 2006. p. 3104–12. Available from: http://pubs.acs.org/doi/pdf/10.1021/ac0351769

35. Lerf A, He H, Forster M, Klinowski J. Structure of graphite oxide revisited. Vol. 102, Journal of Physical Chemistry B. 1998. p. 4477–82.

36. He H, Klinowski J, Forster M, Lerf A. A new structural model for graphite oxide. Vol. 287, Chemical Physics Letters. 1998. p. 53–6.

37. He D, Peng Z, Gong W, Luo Y, Zhao P, Kong L. Mechanism of a green graphene oxide reduction with reusable potassium carbonate. Vol. 5, RSC Advances. 2015. p. 11966–72.

38. Surekha G, Krishnaiah KV, Ravi N, Padma Suvarna R. FTIR, Raman and XRD analysis of graphene oxide films prepared by modified Hummers method. Vol. 1495, Journal of Physics: Conference Series. 2020.

39. Sudesh, Kumar N, Das S, Bernhard C, Varma GD. Effect of graphene oxide doping on superconducting properties of bulk MgB2. Vol. 26, Superconductor Science and Technology. 2013.

40. Osswald S, Flahaut E, Gogotsi Y. In situ raman spectroscopy study of oxidation of double- and single-wall carbon nanotubes. Vol. 18, Chemistry of Materials. 2006. p. 1525–33.

41. Knauer M, Schuster ME, Sn D, Schlögl R, Niessner R, Ivleva NP. Soot structure and reactivity analysis by raman microspectroscopy, temperature-programmed oxidation, and high-resolution transmission electron microscopy. Vol. 113, Journal of Physical Chemistry A. 2009. p. 13871–80.

42. Graf D, Molitor F, Ensslin K, Stampfer C, Jungen A, Hierold C, et al. Spatially resolved raman spectroscopy of single- and few-layer graphene. Vol. 7, Nano Letters. 2007. p. 238–42.

43. Ferrari AC, Basko DM. Raman spectroscopy as a versatile tool for studying the properties of graphene. Vol. 8, Nature Nanotechnology. 2013. p. 235–46.

44. Kudin KN, Ozbas B, Schniepp HC, Prud'homme RK, Aksay IA, Car R. Raman spectra of graphite oxide and functionalized graphene sheets. Vol. 8, Nano Letters. 2008. p. 36–41.

45. Zhang X, Kumari G, Heo J, Jain PK. In situ formation of catalytically active graphene in ethylene photo-epoxidation. Vol. 9, Nature Communications. 2018.

46. Kim UJ, Furtado CA, Liu X, Chen G, Eklund PC. Raman and IR spectroscopy of chemically processed single-walled carbon nanotubes. Vol. 127, Journal of the American Chemical Society. 2005. p. 15437–45.

47. Ni Z, Wang Y, Yu T, Shen Z. Raman spectroscopy and imaging of graphene. Vol. 1, Nano Research. 2008. p. 273–91.

48. Pimenta MA, Dresselhaus G, Dresselhaus MS, Cançado LG, Jorio A, Saito R. Studying disorder in graphite-based systems by Raman spectroscopy. Vol. 9, Physical Chemistry Chemical Physics. 2007. p. 1276–91.

49. Filik J, May PW, Pearce SRJ, Wild RK, Hallam KR. XPS and laser Raman analysis of hydrogenated amorphous carbon films. Vol. 12, Diamond and Related Materials. 2003. p. 974–8.

50. Lv Q, Si W, He J, Sun L, Zhang C, Wang N, et al. Selectively nitrogen-doped carbon materials as superior metal-free catalysts for oxygen reduction. Vol. 9, Nature Communications. 2018.

51. Lesiak B, Stobinski L, Kövér L, Tóth J, Kurzydłowski KJ. Ar ion bombardment modification of Pd-Au/MWCNTs catalyst surfaces studied by electron spectroscopy. Phys Status Solidi Appl Mater Sci. 2011;208(8):1791–5.

52. Estrade-Szwarckopf H. XPS photoemission in carbonaceous materials: A “defect” peak beside the graphitic asymmetric peak. Vol. 42, Carbon. 2004. p. 1713–21.

53. Kwan YCG, Ng GM, Huan CHA. Identification of functional groups and determination of carboxyl formation temperature in graphene oxide using the XPS O 1s spectrum. Vol. 590, Thin Solid Films. 2015. p. 40–8.

54. Azari S, Karimi M, Kish MH. Structural properties of the Poly(acrylonitrile) membrane prepared with different cast thicknesses. Ind Eng Chem Res. 2010;49(5):2442–8.

55. Vandezande P, Li X, Gevers LEM, Vankelecom IFJ. High throughput study of phase inversion parameters for polyimide-based SRNF membranes. Vol. 330, Journal of Membrane Science. 2009. p. 307–18.

56. Vandezande P, Gevers LEM, Vankelecom IFJ. Solvent resistant nanofiltration: Separating on a molecular level. Vol. 37, Chemical Society Reviews. 2008. p. 365–405.

57. Soroko I, Sairam M, Livingston AG. The effect of membrane formation parameters on performance of polyimide membranes for organic solvent nanofiltration (OSN). Part C. Effect of polyimide characteristics. Vol. 381, Journal of Membrane Science. 2011. p. 172–82.

58. Hołda AK, Vankelecom IFJ. Understanding and guiding the phase inversion process for synthesis of solvent resistant nanofiltration membranes. J Appl Polym Sci. 2015;132(27):1–17.